NON-PERTURBATIVE AND TOPOLOGICAL ASPECTS OF QCD — 30th May 2024

QCD Instanton Prospects at the LHC

Ynyr Harris

In This Talk

- Present ongoing search for gluon-induced QCD instantons in ATLAS
  - Based on work done by V. V. Khoze *et al.* (see previous talk)
  - Very ATLAS oriented
  - A work in progress! No data will be shown.

- But it is difficult! Are there other avenues?
  - Diffractive production?
  - Use flavour tagging?
  - Measure the chirality violation?

Following 't Hooft, do perturbation theory in the instanton background

[Khoze *et al.* 1] + [Khoze *et al.* 2, Khoze *et al.* 3, Amoroso *et al.*]

$$\mathcal{A}_{2\to n_g+2N_f} = \int d^4x_0 \int_0^\infty d\rho\, D(\rho)\, e^{-S_I} \prod_{i=1}^{n_g+2} A_{\mathrm{LSZ}}^{\mathrm{inst}}(p_i;\rho) \prod_{j=1}^{2N_f} \psi_{\mathrm{LSZ}}^{(0)}(p_j;\rho)$$

Event signature

Get cross-section via optical theorem

$$\hat{\sigma}(gg \to X) = \frac{1}{E^2} \mathrm{Im}\mathcal{A}^{I\bar{I}}$$

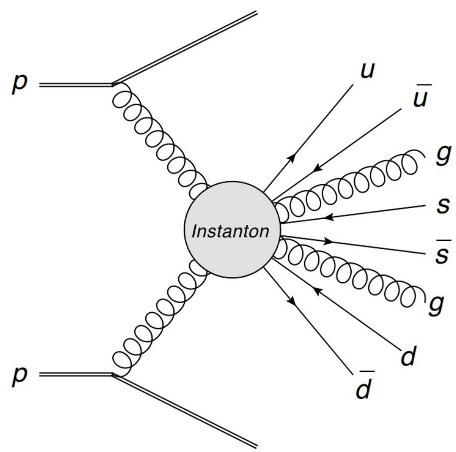

Predictions for the LHC

$\sqrt{\hat{s}}$ [GeV]	$\hat{\sigma}(gg \to X)$ [pb]	$\langle 1/\rho \rangle$ [GeV]	$\alpha_S(1/\rho)$	$\langle N_{\text{gluons}} \rangle$
20	2.01×10^6	1.69	0.327	7.81
25	9.49×10^5	1.98	0.306	8.58
30	4.64×10^5	2.27	0.290	9.07
35	2.32×10^5	2.52	0.279	9.61
40	1.25×10^5	2.84	0.267	9.67
50	3.89×10^4	3.38	0.251	10.56
60	1.38×10^4	3.87	0.241	10.89
70	5.45×10^3	4.33	0.232	11.38
80	2.36×10^3	4.85	0.224	11.67
90	1.08×10^3	5.24	0.219	12.31
100	5.44×10^2	5.82	0.213	12.10
110	2.79×10^2	6.21	0.209	12.62
120	1.53×10^2	6.71	0.205	12.77
130	8.56×10^1	7.13	0.201	13.04
140	4.99×10^1	7.57	0.198	13.25
150	3.01×10^1	8.00	0.195	13.45

Table. Partonic cross-section as a function of partonic centre-of-mass energy, $\sqrt{\hat{s}}$, taken from 2104.01861.

Theory Inputs to an Experimental Search

Nominal factorisation scale choice, μ_F

Mass spectrum

Mean number of gluons to add to each event

$\sqrt{\hat{s}}$ [GeV]	$\hat{\sigma}(gg \to X)$ [pb]	$\langle 1/\rho \rangle$ [GeV]	$\alpha_S(1/\rho)$	$\langle N_{\text{gluons}} \rangle$
20	2.01×10^6	1.69	0.327	7.81
25	9.49×10^5	1.98	0.306	8.58
30	4.64×10^5	2.27	0.290	9.07
35	2.32×10^5	2.52	0.279	9.61
40	1.25×10^5	2.84	0.267	9.67
50	3.89×10^4	3.38	0.251	10.56
60	1.38×10^4	3.87	0.241	10.89
70	5.45×10^3	4.33	0.232	11.38
80	2.36×10^3	4.85	0.224	11.67
90	1.08×10^3	5.24	0.219	12.31
100	5.44×10^2	5.82	0.213	12.10
110	2.79×10^2	6.21	0.209	12.62
120	1.53×10^2	6.71	0.205	12.77
130	8.56×10^1	7.13	0.201	13.04
140	4.99×10^1	7.57	0.198	13.25
150	3.01×10^1	8.00	0.195	13.45

Table. Partonic cross-section as a function of partonic centre-of-mass energy, $\sqrt{\hat{s}}$, taken from 2104.01861.

MC Instanton Signal Modelling

- SHERPA 3 for event generation
- RAMBO for phase-space generation
- Final state assembled algorithmically
- Flavour production scheme:
  - Add up to 5 flavours
  - 20 GeV *c*-production threshold
  - 100 GeV *b*-production threshold
- NNPDF3.0 NNLO with $\mu_F = 1 / \rho$ scale choice

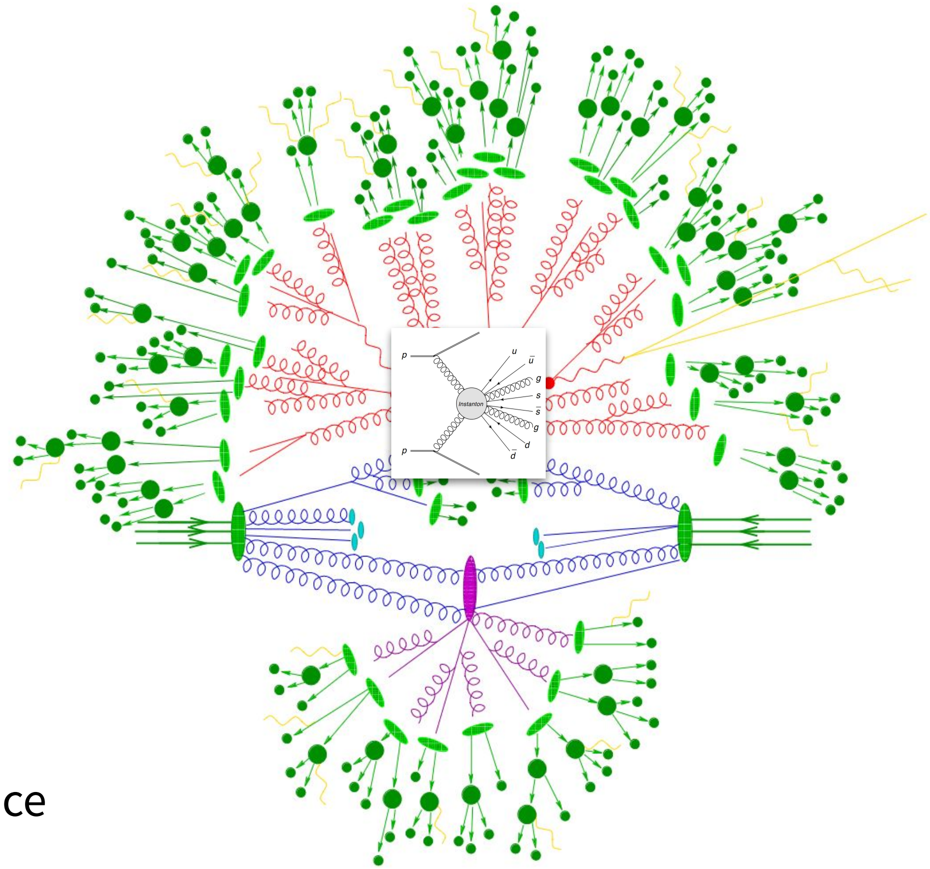

Figure from Sherpa 1.1 Manual ('t Hooft vertex embedded)

See back-up for a glimpse of Sherpa 3's UE tuning effort

Simulated Mass Spectrum

Interpolate the cross-section data table, generate events with Sherpa in 6 slices

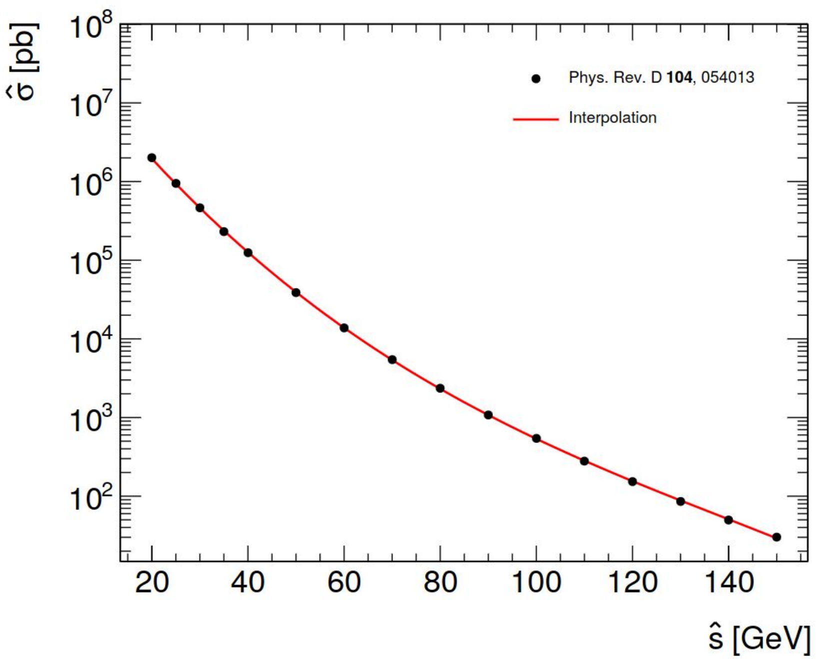

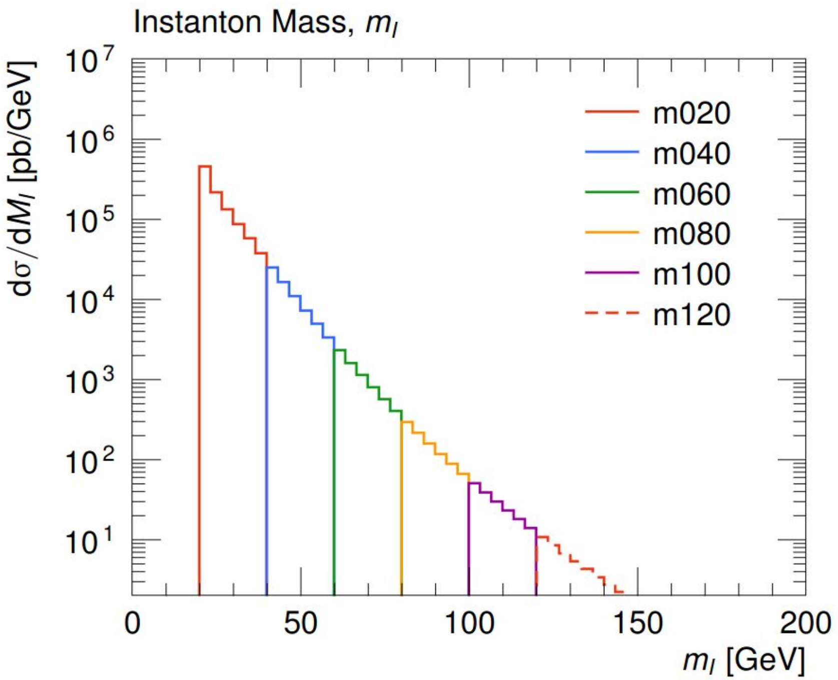

Signal event generator ✔

Soft QCD Background Models

Background: Soft QCD, σ ~ 111 mb

Nominal model: EPOS LHC

Parton-based Gribov Regge theory with collective hadronisation [1306.0121]

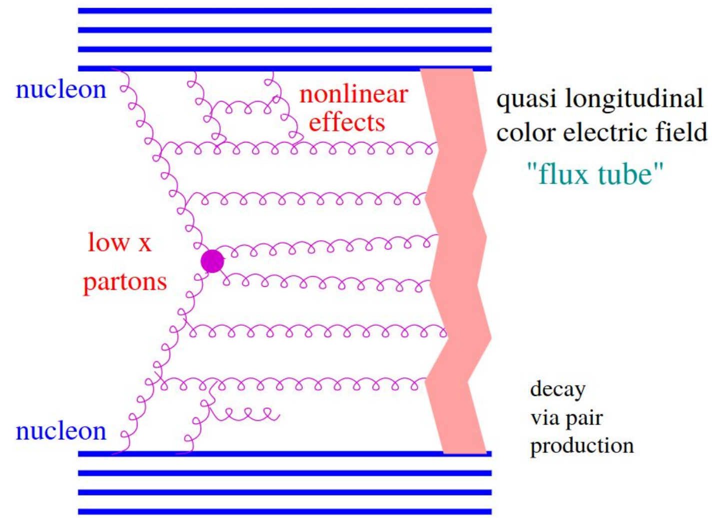

Alternative model: Pythia 8

2 → 2 scatters with MPI based on the Sjöstrand–van Zijl model [PRD], Lund-string fragmentation

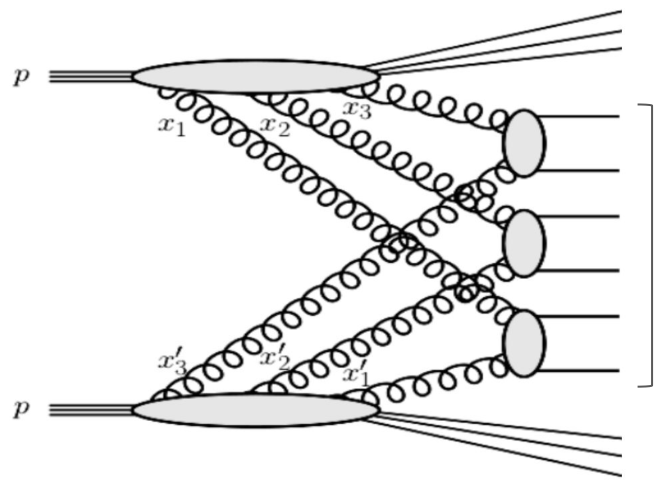

MPI
~ Minimum Bias
[2104.01861]

Start With a Past Analysis

Charged-particle distributions in $\sqrt{s}$ = 13 TeV *pp* interactions measured with the ATLAS detector at the LHC

The ATLAS Collaboration

Featuring

- Low pileup ATLAS data
  - Pile-up values⟨μ⟩~ 0.035
  - 1.693 nb^{-1} ~ $O(10^4)$ instantons
- Minimum Bias triggers
- Charged-particle tracking
- Minimum Bias background models

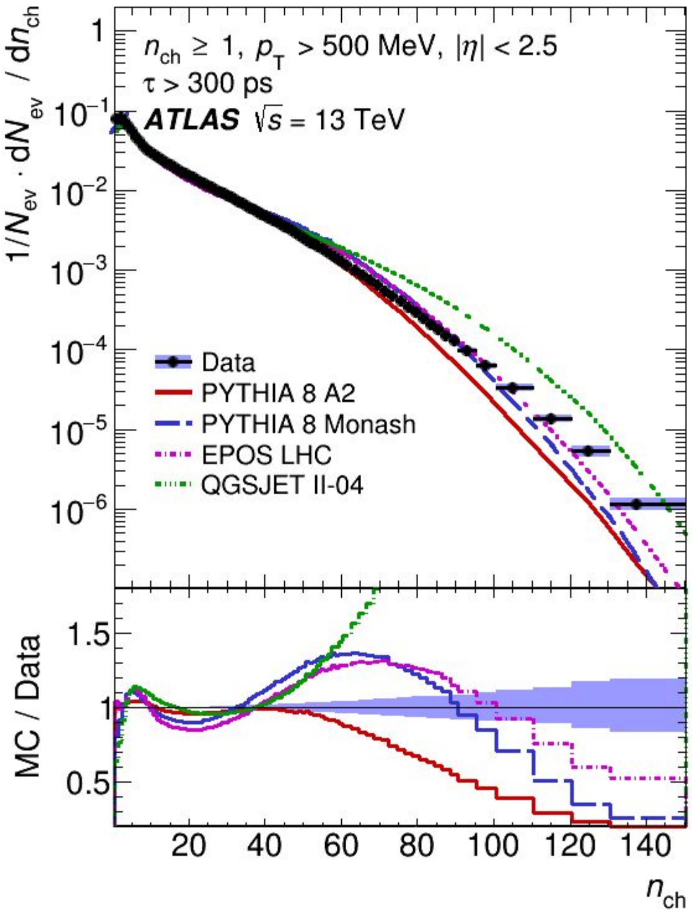

1602.01633

A Very Simple Analysis

- No jets, flavour tagging, heavy decays, … just tracks.

- Good track reconstruction efficiency
- Small systematic uncertainties
- Enough information to capture isotropy
- Simplified analysis design

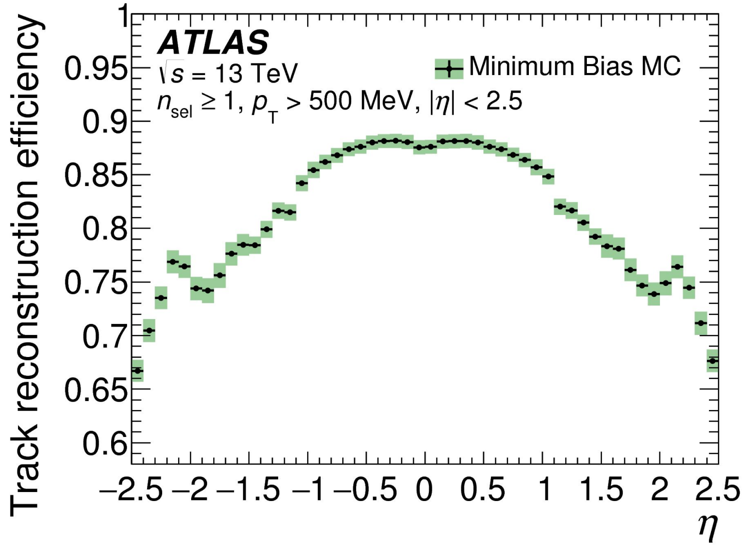

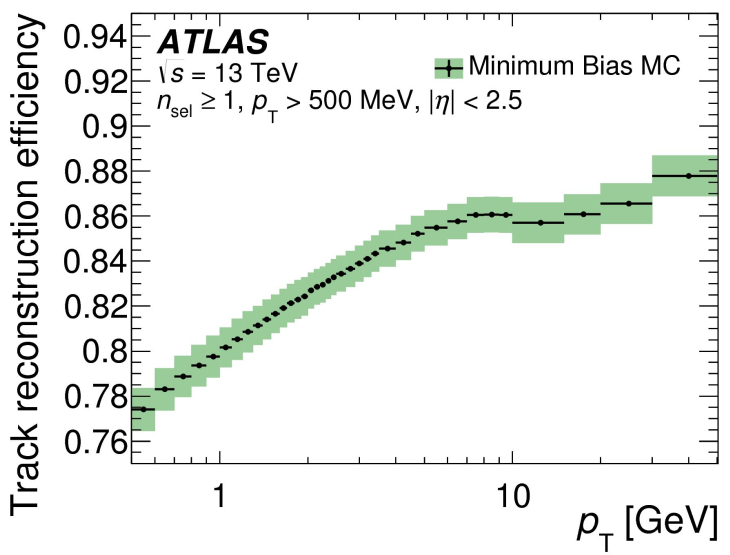

1602.01633

Discriminating Variables
— Event kinematics

Variable
Track multiplicity
Scalar sum of p_{T}
Leading track-p_{T}
Number of high-p_{T} tracks
Number of low-p_{T} tracks
Mean p_{T}
Median p_{T}
Transverse mass
Transverse mass per track
Mean η
Standard deviation of ϕ
Standard deviation of η
Standard deviation of $\Delta\phi(i, j)$ of all track pairs
Standard deviation of $\Delta\eta(i, j)$ of all track pairs
Mean of $\lvert\Delta\eta(i, j)\rvert$ of all track pairs

Variables roughly proportional to event mass

Variables inspired by two-particle azimuthal correlation studies in Heavy Ion data [eg 2101.10771]

Discriminating Variables

— Event kinematics

Variable
Track multiplicity
Scalar sum of p_T
Leading track-p_T
Number of high-p_T tracks
Number of low-p_T tracks
Mean p_T
Median p_T
Transverse mass
Transverse mass per track
Mean η
Standard deviation of ϕ
Standard deviation of η
Standard deviation of $\Delta\phi(i, j)$ of all track pairs
Standard deviation of $\Delta\eta(i, j)$ of all track pairs
Mean of $\|\Delta\eta(i, j)\|$ of all track pairs

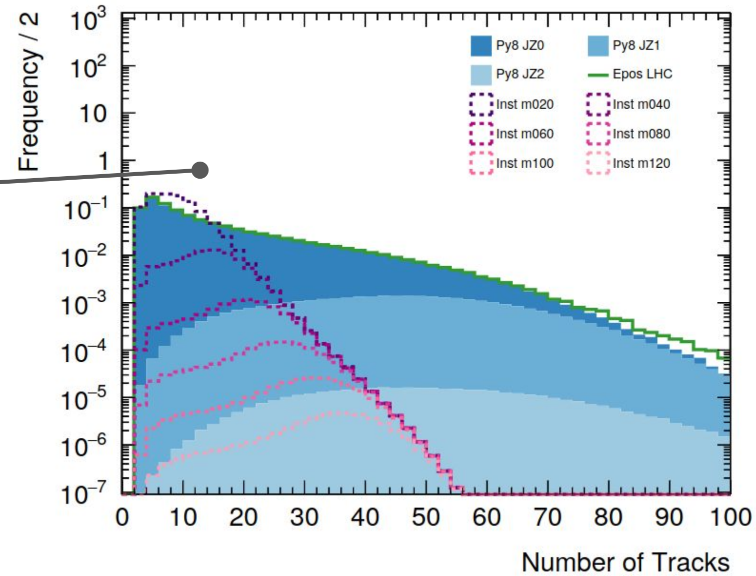

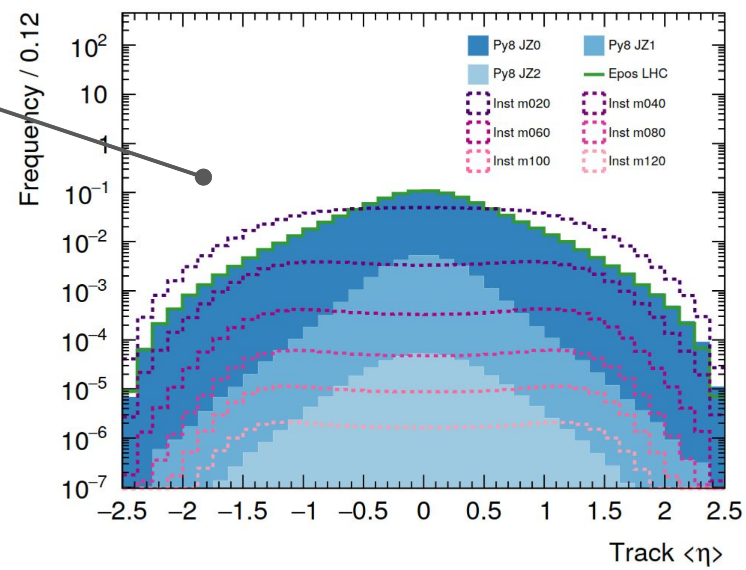

Discriminating Variables
— Event Shapes

Thrust:

$$T(X) = \max_{e_T} \frac{\sum_i |e_T \cdot x_i|}{\sum_i |x_i|}$$

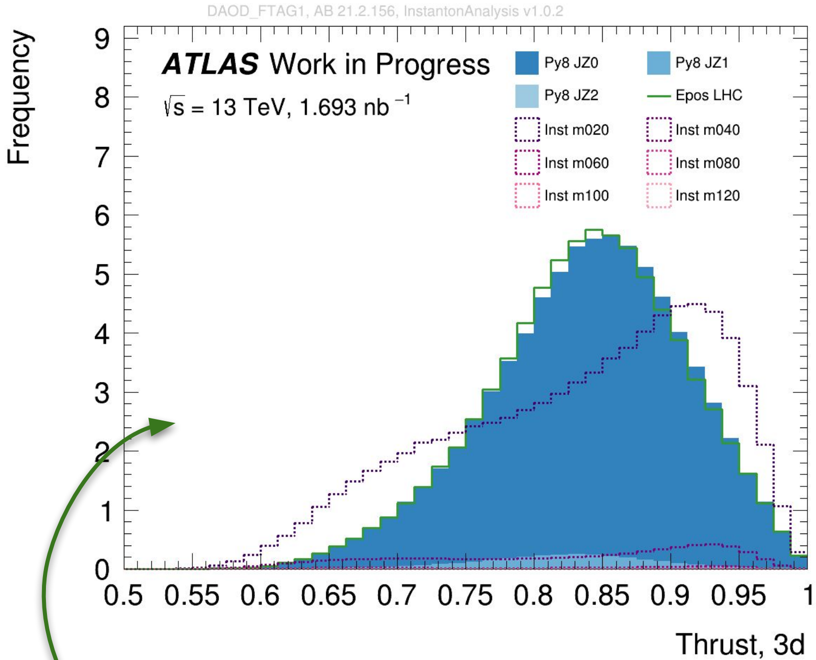

Sphericity:

$$S^{\alpha\beta}(X;r) = \frac{\sum_i |x_i|^{r-2} x_i^\alpha x_i^\beta}{\sum_i |x_i|^r}$$

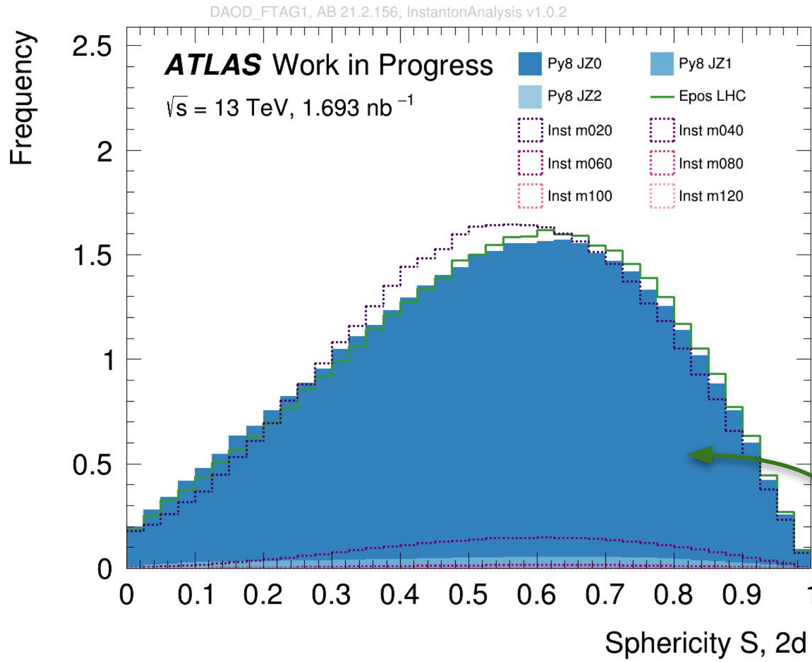

3d distributions depend on Björken-x combinations and minimum track p_T cut (500 MeV)

Very similar distributions in 2d (similar features in 3d)

Discriminating Variables
— Flatenicity

- 'Flatenicity' characterises the uniformity of energy deposits in the detector [2204.13733]
- Sensitive to the number of MPI interactions
- η — ϕ plane partitioned into a uniform 10 x 10 grid of cells
- Total track pT in each cell calculated…then flatenicity given by

$$\rho = \frac{\sigma_{p_{\mathrm{T}}^{\mathrm{cell}}}}{\langle p_{\mathrm{T}}^{\mathrm{cell}} \rangle}$$

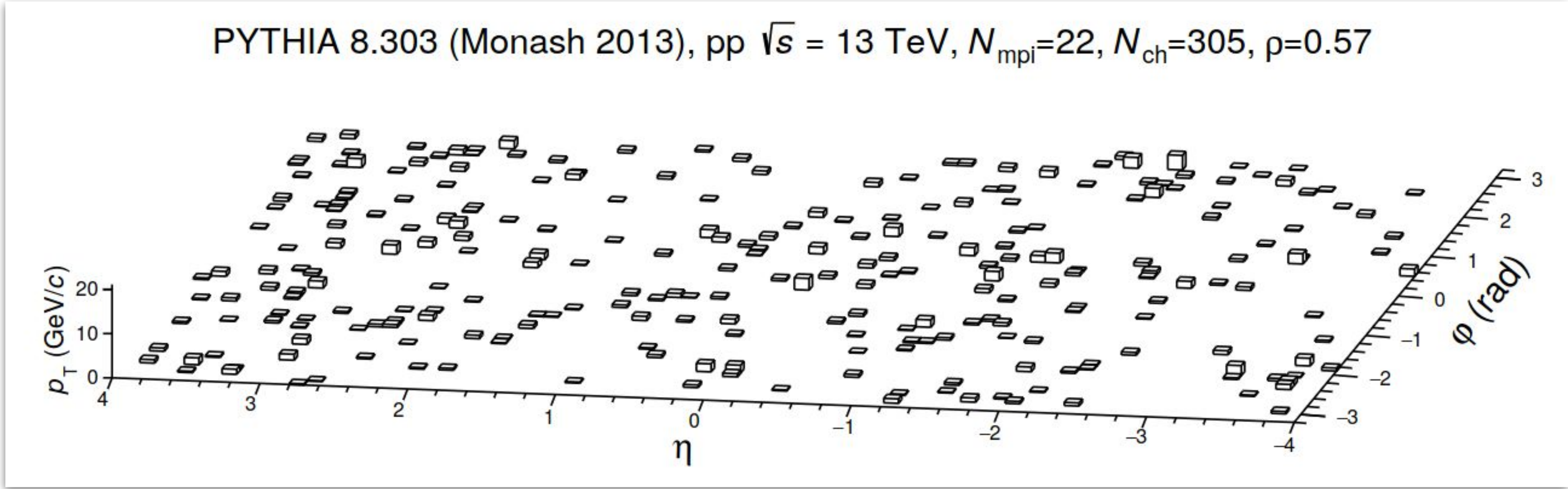

Picture of a uniform 'MPI' event taken from [2204.13733]

Correlation Matrices

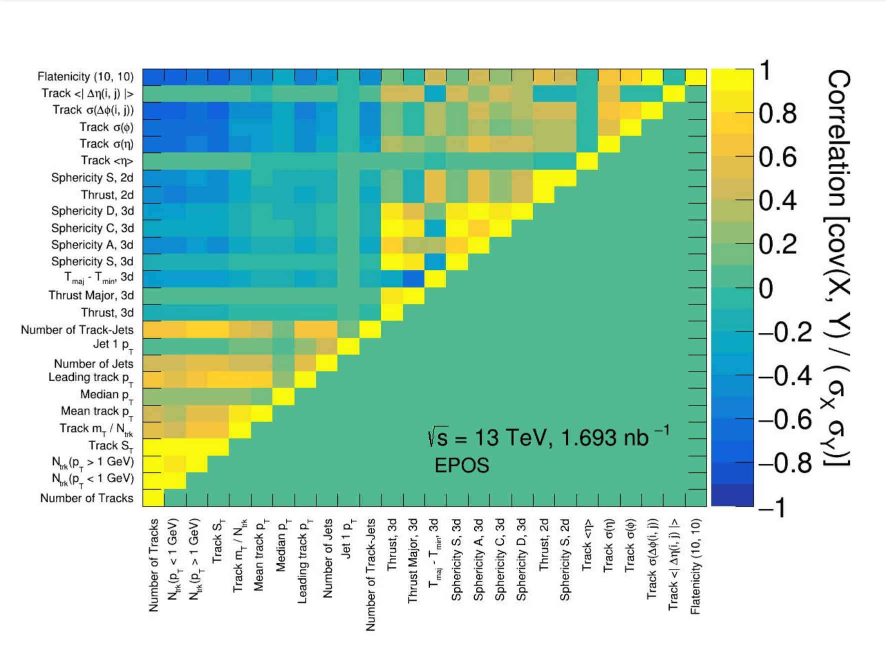

EPOS LHC

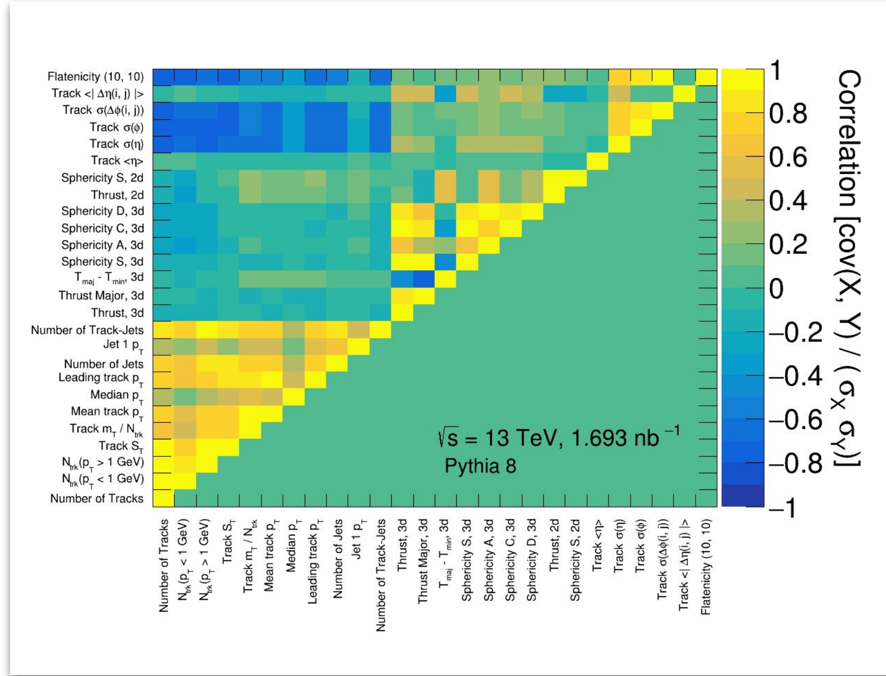

Pythia 8

These matrices factorise into two blocks: Event Shapes and non Event-Shapes

For background estimation, find two independent variables for the ‘ABCD’ method?

Machine Learning Approach: ABCDisCo

Set up two statistically independent classifiers for ABCD-style background estimation

[Kasieczka, Nachman, Schwartz and Shih (2007.14400)]

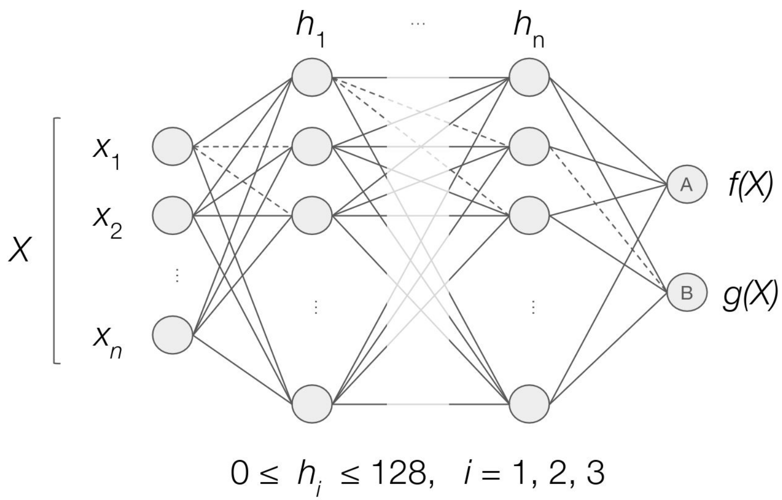

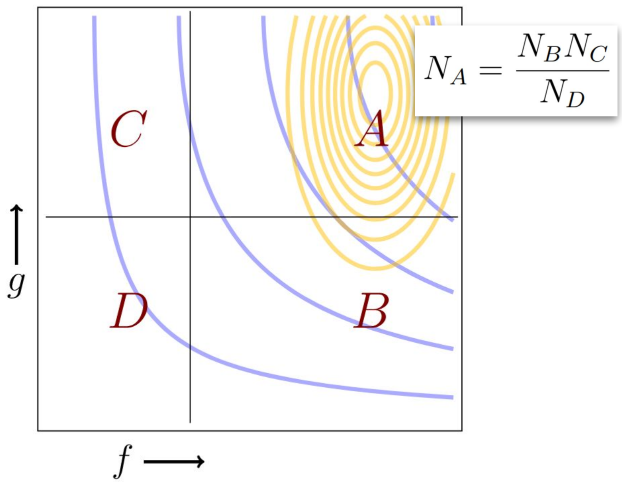

$$\mathcal{L}[f(X), g(X)] = \mathcal{L}_{\text{cl}}[f(X), y] + \mathcal{L}_{\text{cl}}[g(X), y] + \alpha\, \mathcal{L}_{\text{dCorr}^2_{y=0}}[f(X), g(X)]$$

Classification terms

Decorrelation term, strength α

Modified loss function

→ Region definitions and background estimation

Deep Neural Network (DNN) Input Variables

Mass variables	Number of tracks	N_{trk}
	Number of tracks above 1 GeV	$N_{\text{trk}}(p_{\text{T}} > 1\,\text{GeV})$
	Number of tracks below 1 GeV	$N_{\text{trk}}(p_{\text{T}} < 1\,\text{GeV})$
	Scalar sum of track p_{T}	S_T
	Transverse mass per track	m_T / N_{trk}
	Mean track p_{T}	$\langle p_{\text{T}} \rangle$
	Median track p_{T}	med p_{T}
	Leading track p_{T}	max p_{T}
Event Shape variables	$3d$ Thrust	$T, 3d$
	$3d$ Thrust major	$T_{\text{major}}, 3d$
	$3d$ Oblateness	$T_{\text{major}} - T_{\text{minor}}, 3d$
	$3d$ Sphericity	$S, 3d$
	$3d$ Aplanarity	$A, 3d$
	$2d$ Thrust	$T, 2d$
	$2d$ Sphericity	$S, 2d$
Angular variables	Mean pseudorapidity	$\langle \eta \rangle$
	Standard deviation of ϕ	$\sigma(\phi)$
	Standard deviation of η	$\sigma(\eta)$
	Standard deviation of $\Delta\phi(i,j)$ of all track pairs	$\sigma(\Delta\phi(i,j))$
	Mean of $\lvert\Delta\eta(i,j)\rvert$ of all track pairs	$\langle \lvert\Delta\eta(i,j)\rvert \rangle$
	Flatenicity on a 10×10 grid	$F(10,10)$

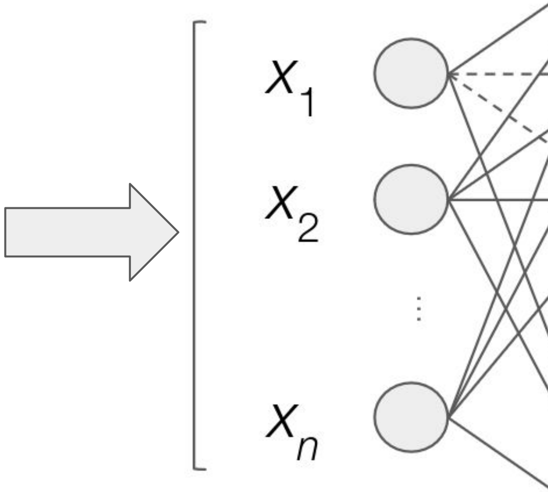

Table. List of our ABCDisCo network input variables.

“Mass” Binning

Proxy for instanton mass

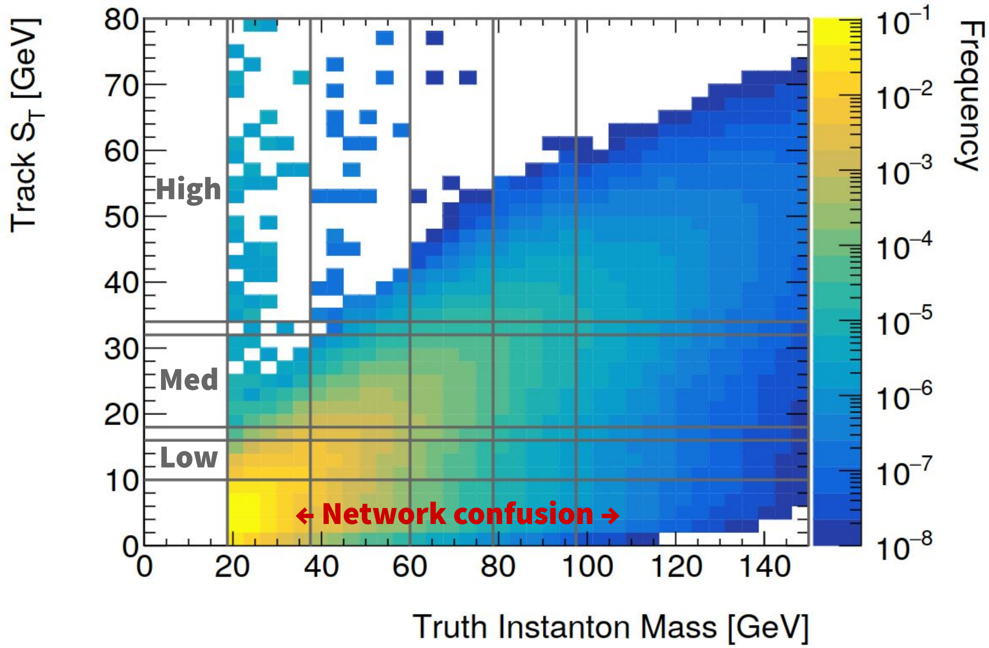

Define 3 bins by optimising efficiency x purity

Truth mass bins: (20, 40), (100, 150), (60, 80) GeV

- Principled choice: do the analysis in reconstructed mass bins
  - Decouple somewhat from cross-section modelling
  - Enhance sensitivity with a shape fit
  - Also, it aids the DNN training

Classifier Output Planes (Or ‘ABCD’ Planes)

Background (EPOS)

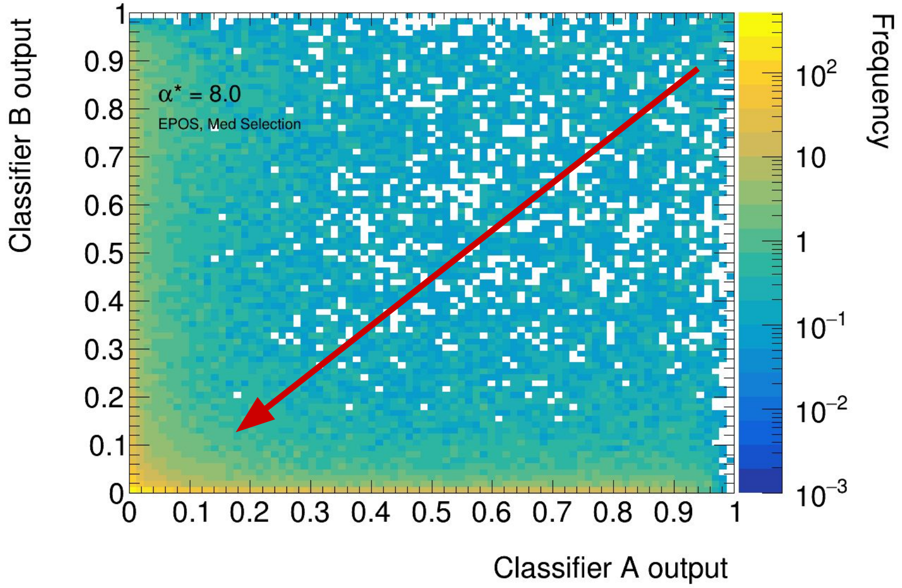

Signal

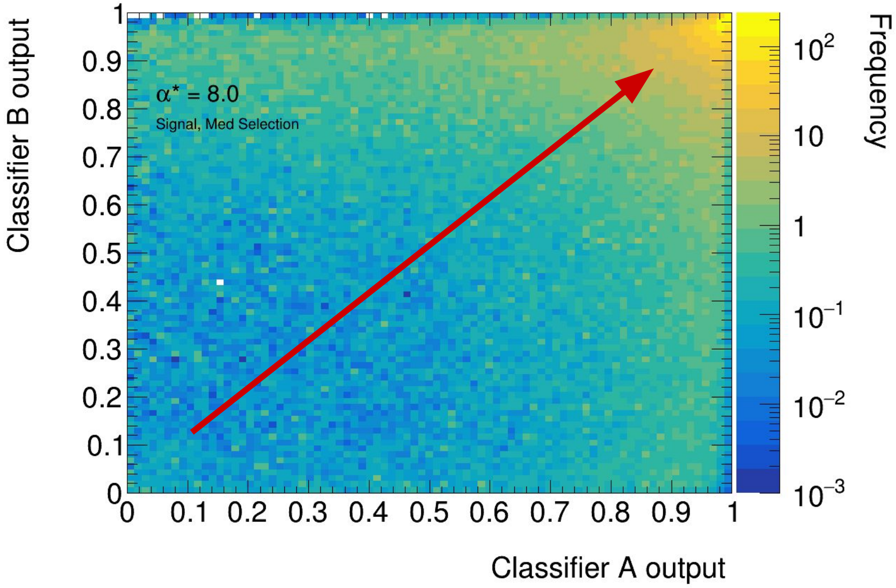

Classifier Output Distributions: Low Mass

Background ←

Signal →

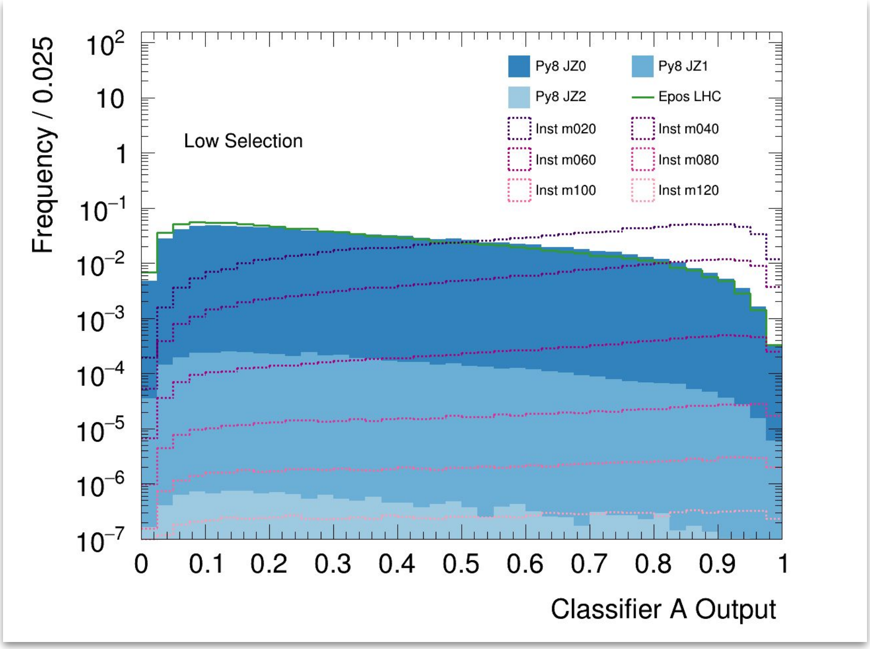

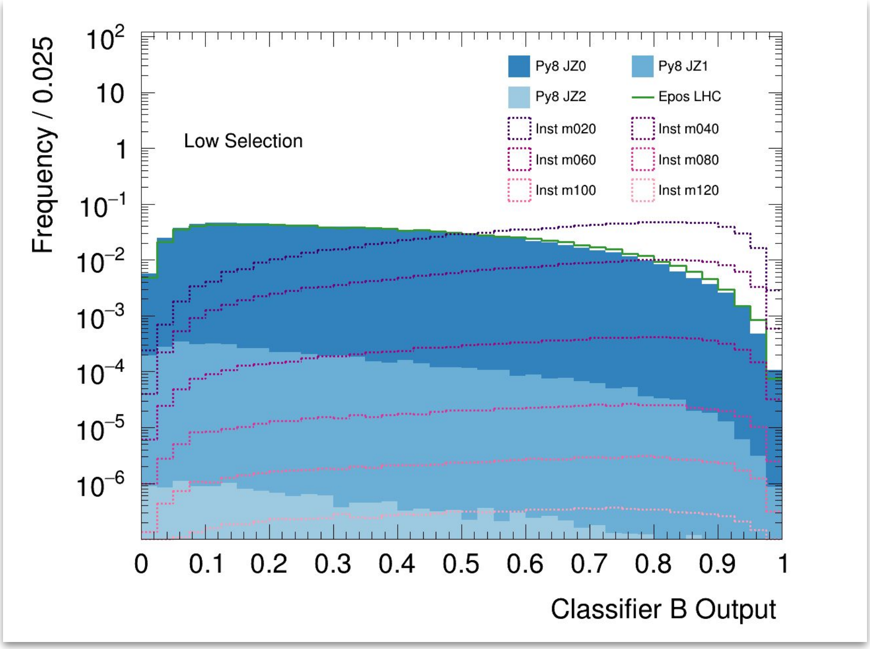

Classifier Output Distributions: Medium Mass

Background ←

Signal →

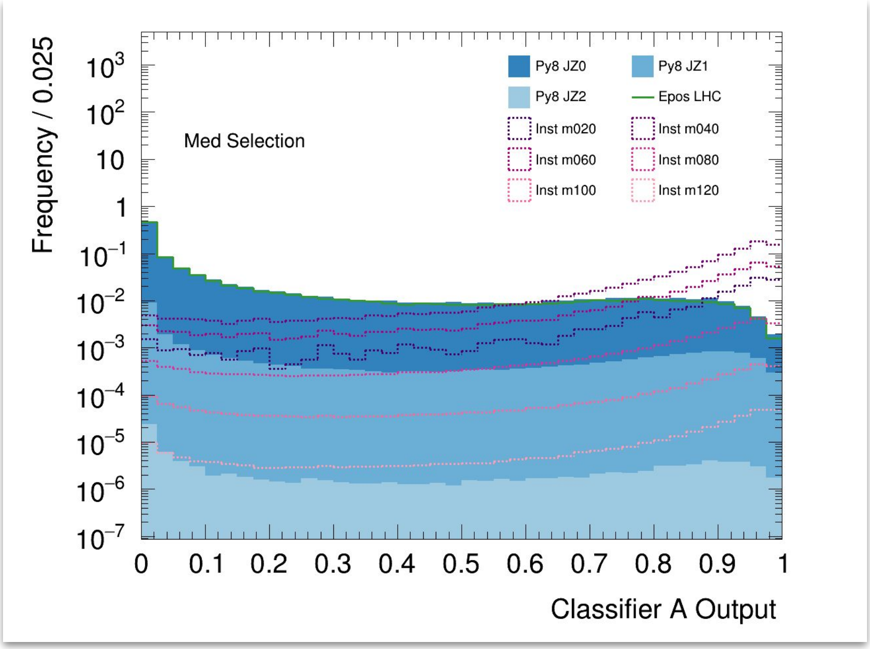

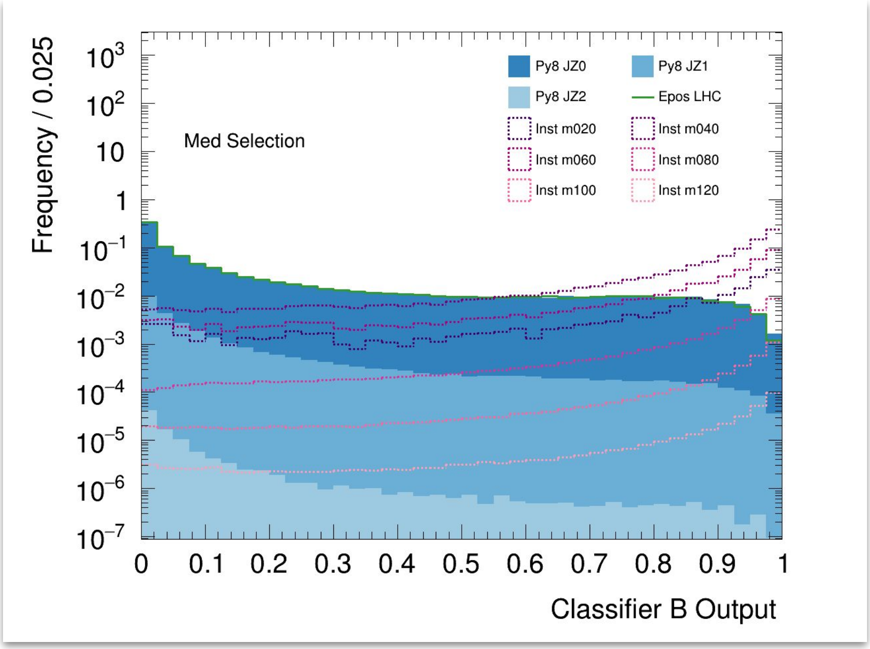

Classifier Output Distributions: High Mass

← Background

Signal →

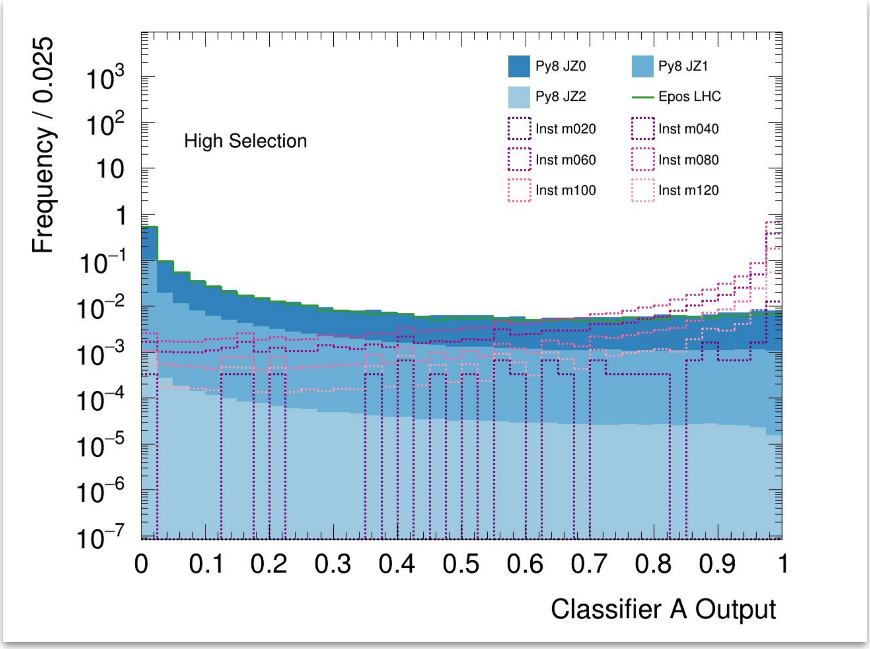

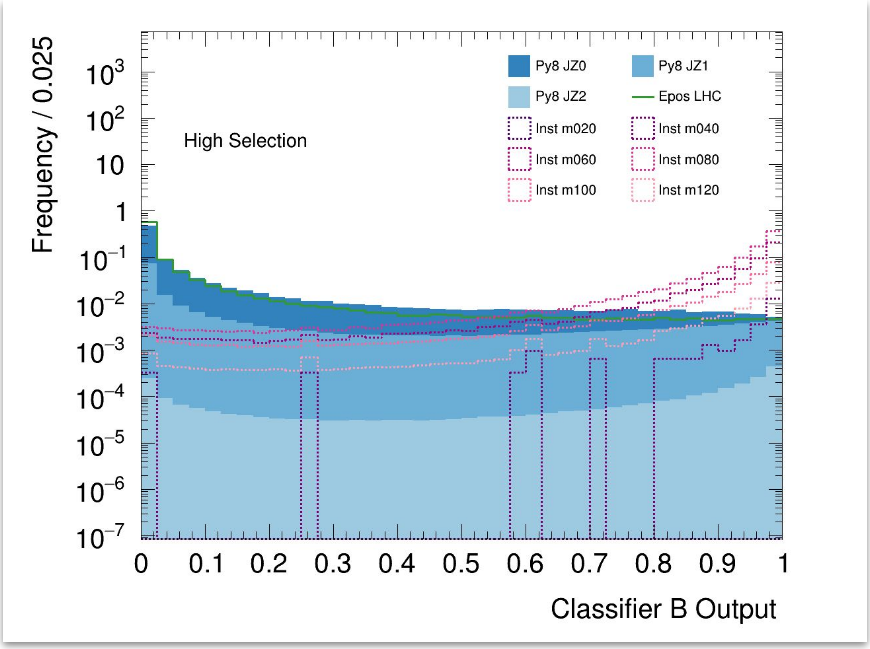

→ Pretty good! But how good?

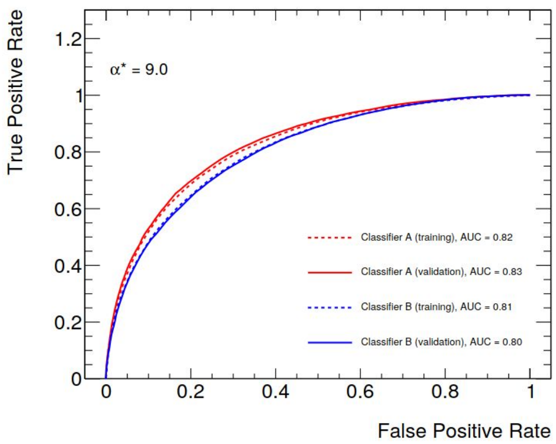

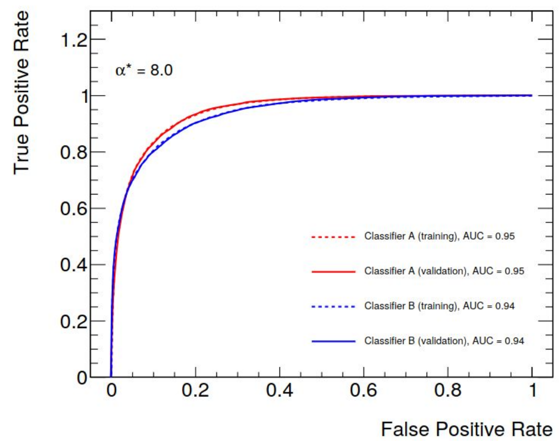

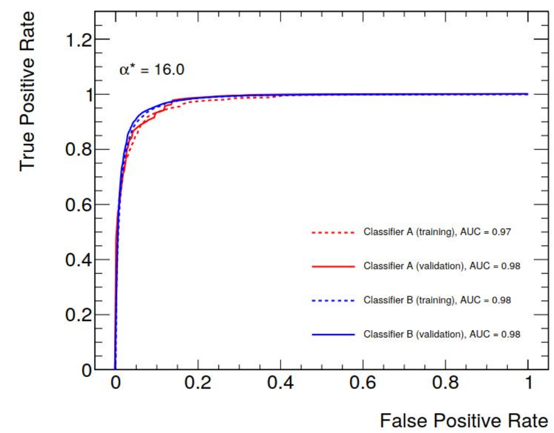

Low-mass

Optimal α = 9

Mean AUC* = 0.82

Medium-mass

Optimal α = 8

Mean AUC = 0.95

High-high

Optimal α = 16

Mean AUC = 0.98

Classification performance improves from low to high-mass

*Area Under the [ROC] Curve (AUC)

A Particularly Interesting Variable: ⟨|Δη(i, j)|⟩

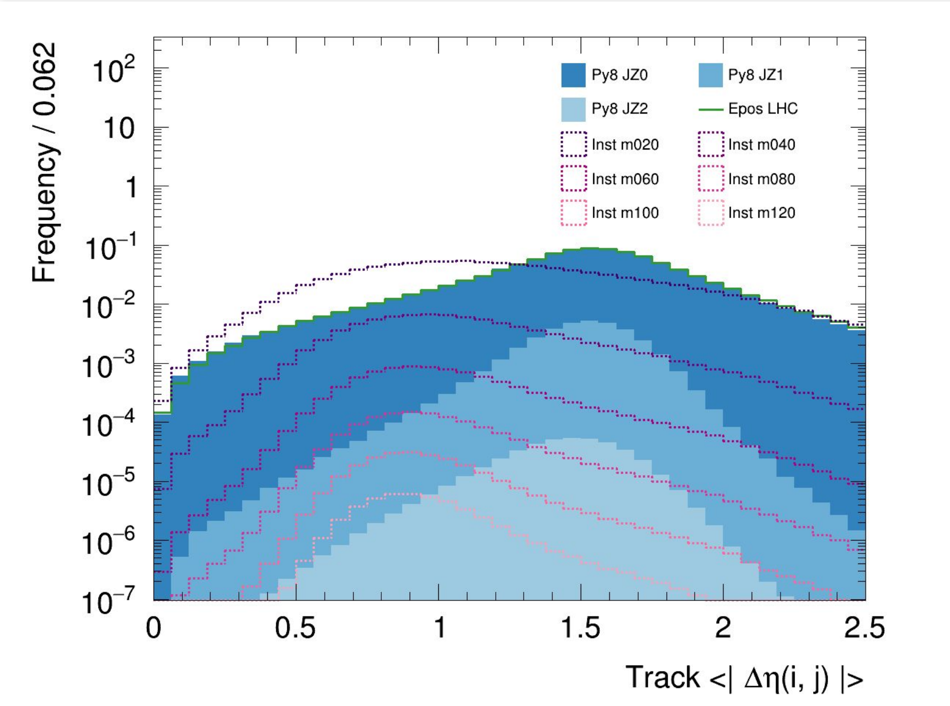

- Mean magnitude of Δη over all pairs of tracks
- Immediately important for the classifiers (right)
- **Captures the so-called ‘instanton band’**
  - T. Carli et al., 'Soft Bombs' paper (2016)

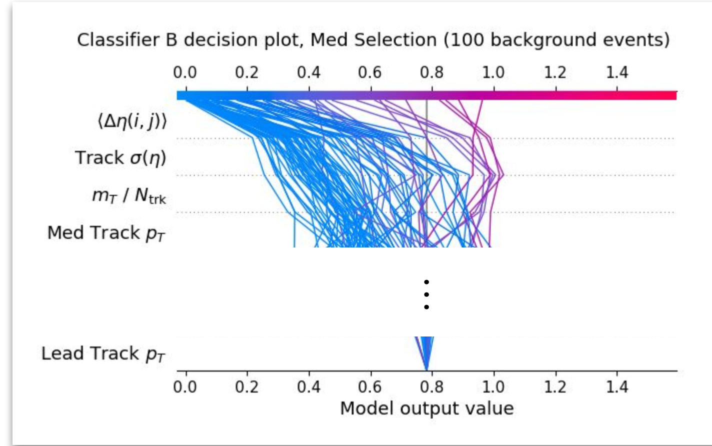

^Network input variable-ranking plot based on SHAP values

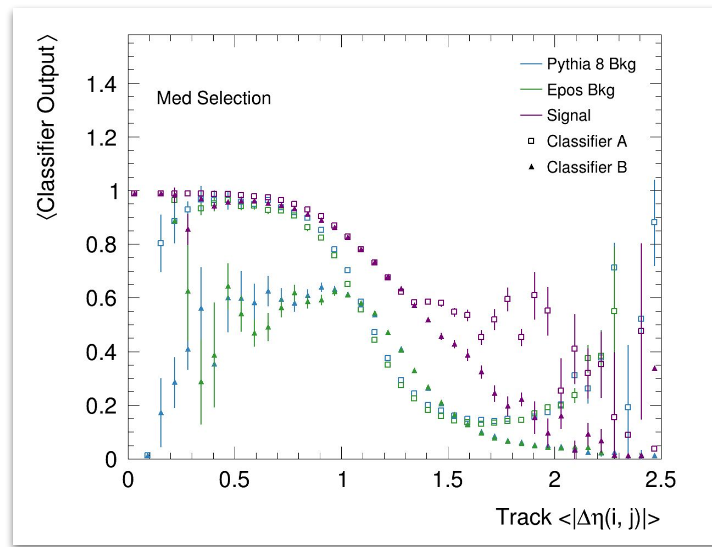

^Mean classifier outputs as functions of the input

‘Instanton Band’ Idea

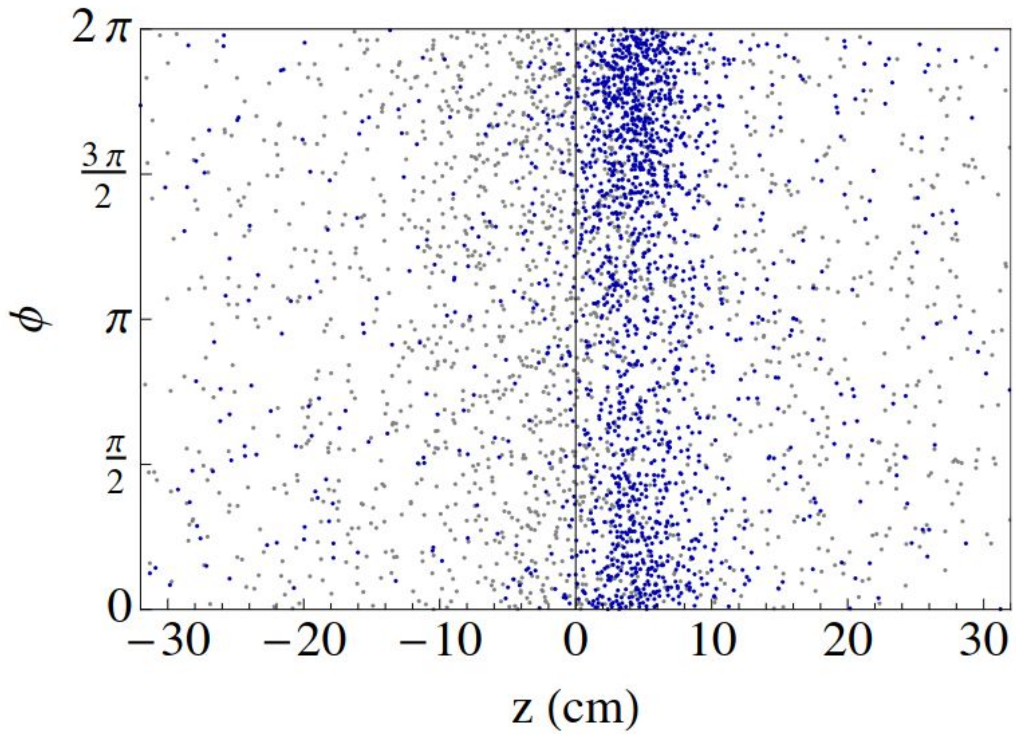

$$\eta = -\ln\left(\tan\frac{\theta}{2}\right)$$

Figure from 1612.00850

- Isotropy in polar angles → band in pseudorapidity (or z in the figure)
- Longitudinal boost of the centre of mass → displacement along z
- More activity concentrated in the band in signal events!
- The DNNs seek out the ‘instanton band’ using the $\langle|\Delta\eta(i,j)|\rangle$ variable!

Background Model Reweighting / “Tracking Corrections”

How to deal with mis-modelling of network inputs?

Somehow reweight MC to data. A procedure that seems to work: reweight the track multiplicity distribution, then reweight the track $p_T - \eta$ distribution in n_{ch} bins.

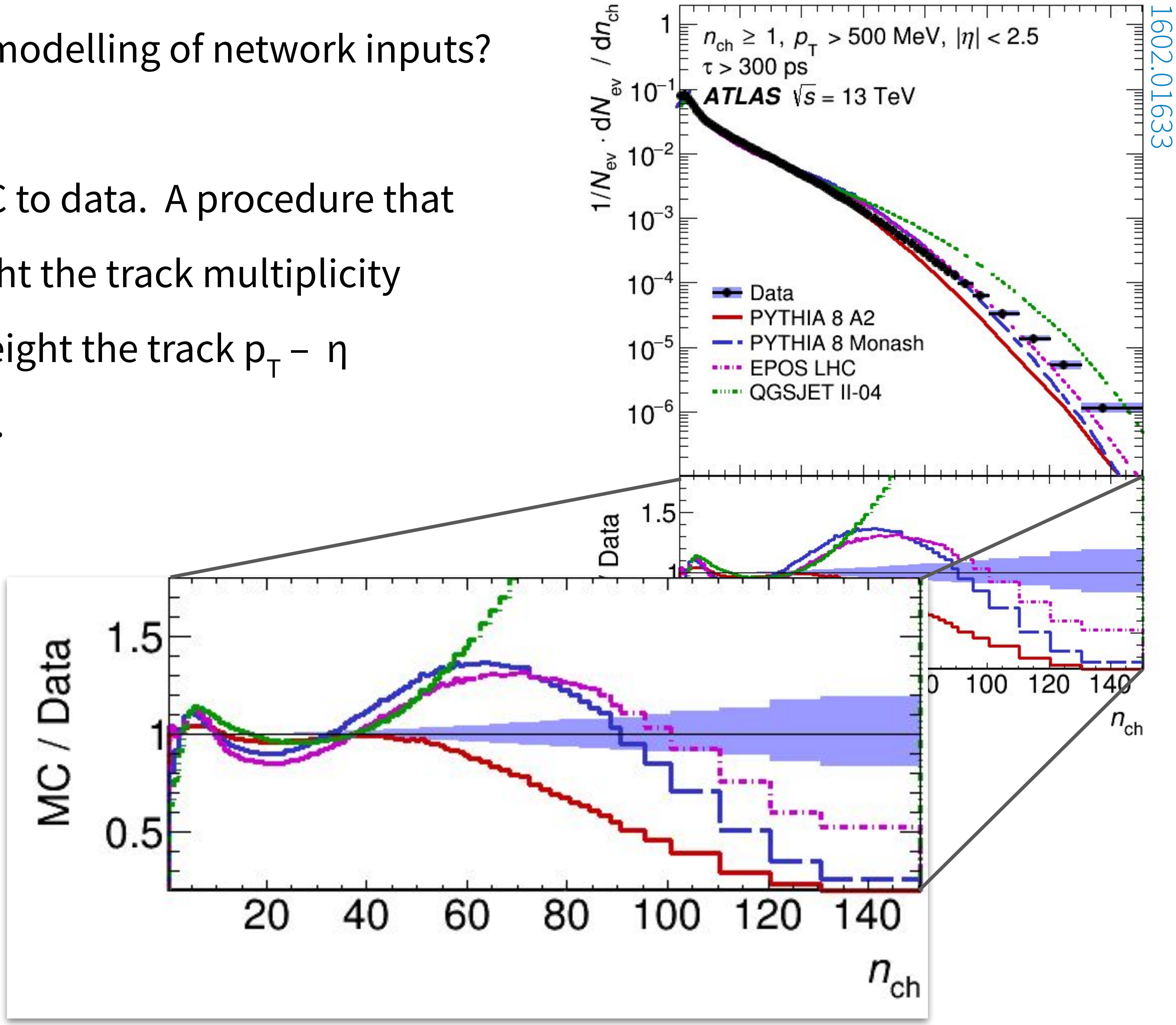

The Principle of Our Background Estimation

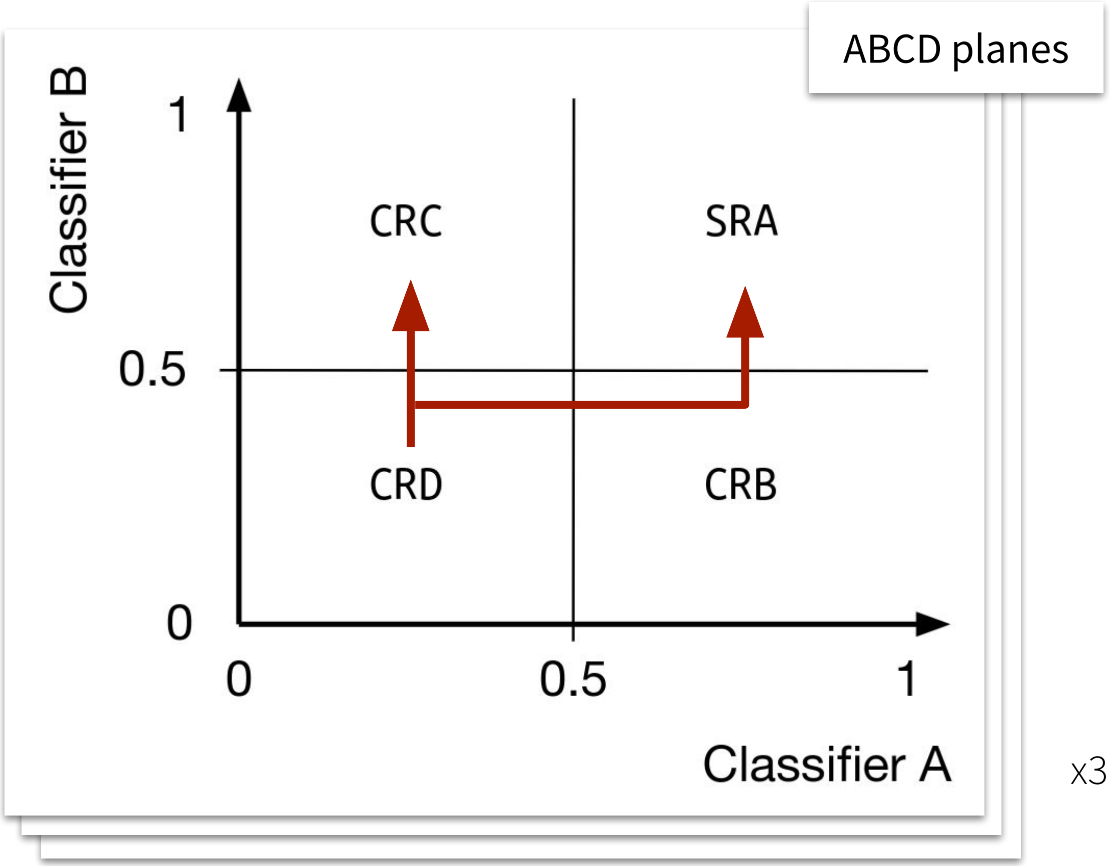

The ABCD equation:

$$N_{BCD} = \frac{N_B \times N_C}{N_D}$$

x3 mass categories

Statistical Analysis: One-Bin Counting Experiment

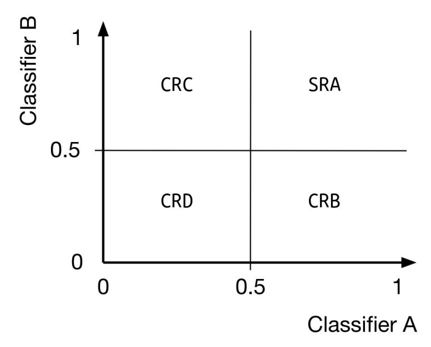

- Three mass categories, and ABCD regions in each
- Standard ATLAS treatment based on a profile likelihood ratio
  - One-bin cut-and-count analysis in each mass category
  - Simple extension: statistical combination

$$L(\mu, \boldsymbol{\theta}) = P_{\mathrm{SR}} \times P_{\mathrm{CR}} \times C_{\mathrm{syst}}$$
$$= \prod_{i=1}^{N} \mathrm{Poiss}(n_i \mid \lambda_i(\mu, \boldsymbol{\theta})) \times \prod_{j=1}^{M} \mathrm{Poiss}(m_j \mid \lambda_j(\mu, \boldsymbol{\theta})) \times C_{\mathrm{syst}}(\boldsymbol{\theta}^0, \boldsymbol{\theta})$$

***N* SRs**

***M* CRs**

NPs
Representing fit parameters and systematic uncertainties

ATLAS Results

< Insert ATLAS results here >

(Spoiler: expected sensitivity is currently not fantastic)

The Main Problem: Irreducible 'Minimum Bias' Background

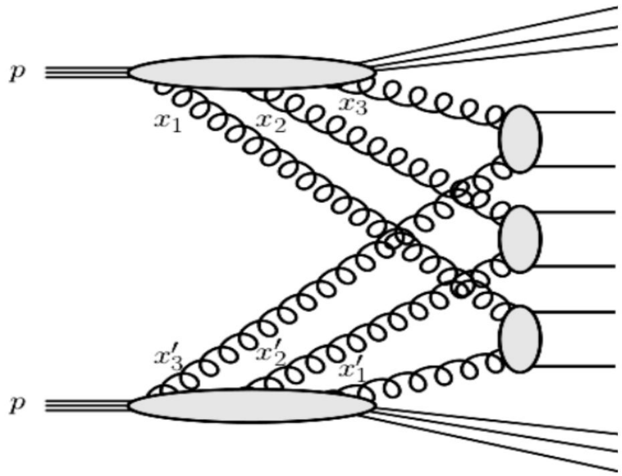

vs

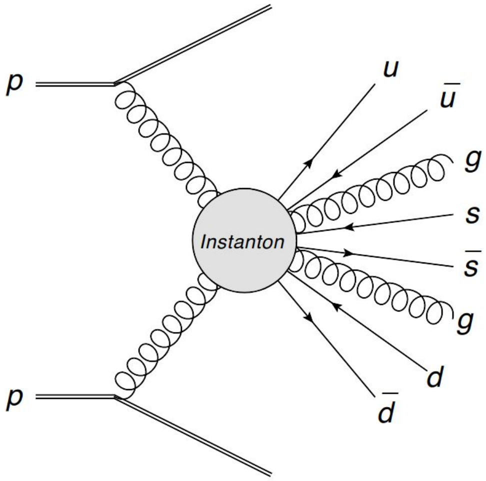

Minimum Bias background | **Instanton signal**

σ ~ 111 mb **vs** **σ ~ 26 μb** **S / B ~ O(10^{-5})**

Signal and background final state kinematics are *very similar*

And the small S / B is difficult to combat (even with our DNNs)

Other Production Modes? Central Exclusive Production…?

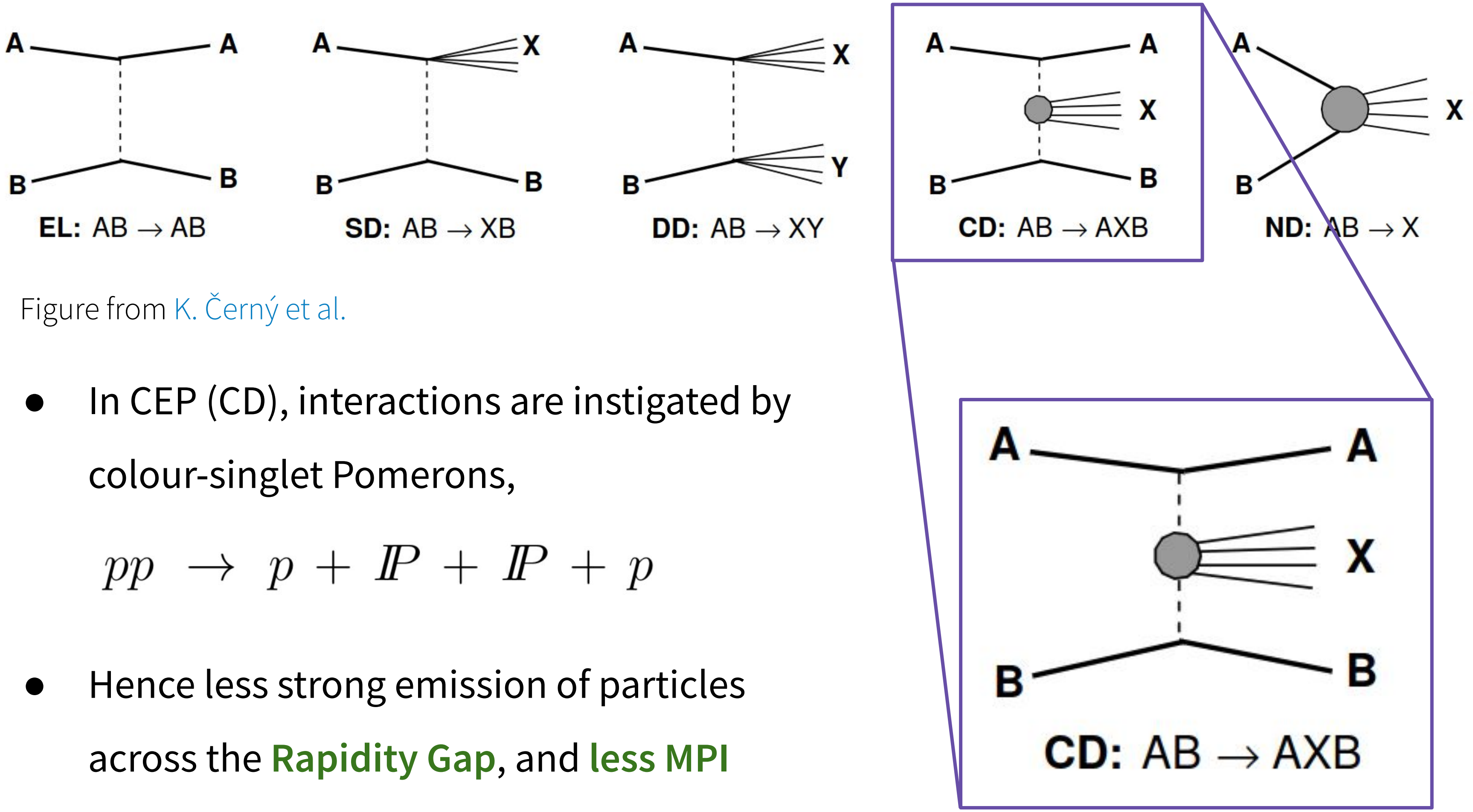

Figure from K. Černý et al.

- In CEP (CD), interactions are instigated by colour-singlet Pomerons,

$$pp \rightarrow p + I\!\!P + I\!\!P + p$$

- Hence less strong emission of particles across the **Rapidity Gap**, and **less MPI background**

V. V. Khoze *et al*. again [PRD **104**, 054013 (2021), PRD **105**, 036008 (2022)]

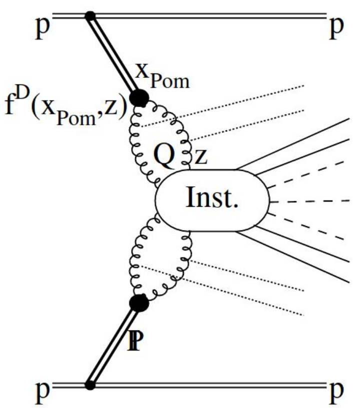

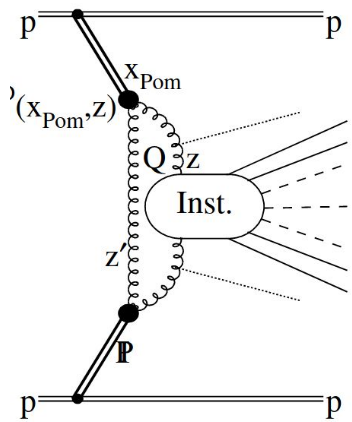

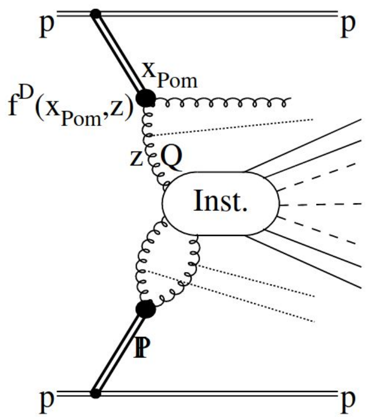

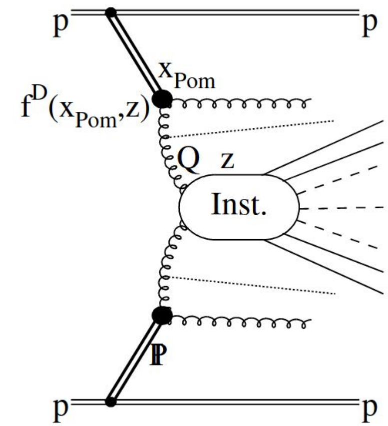

Dominant

- Same calculational technique as for the $gg \rightarrow X$ cross-section
- Cross-sections of up to 10^5 pb for [very] low masses [with no Q_t cut]

CEP is a Possible Search Avenue For ATLAS

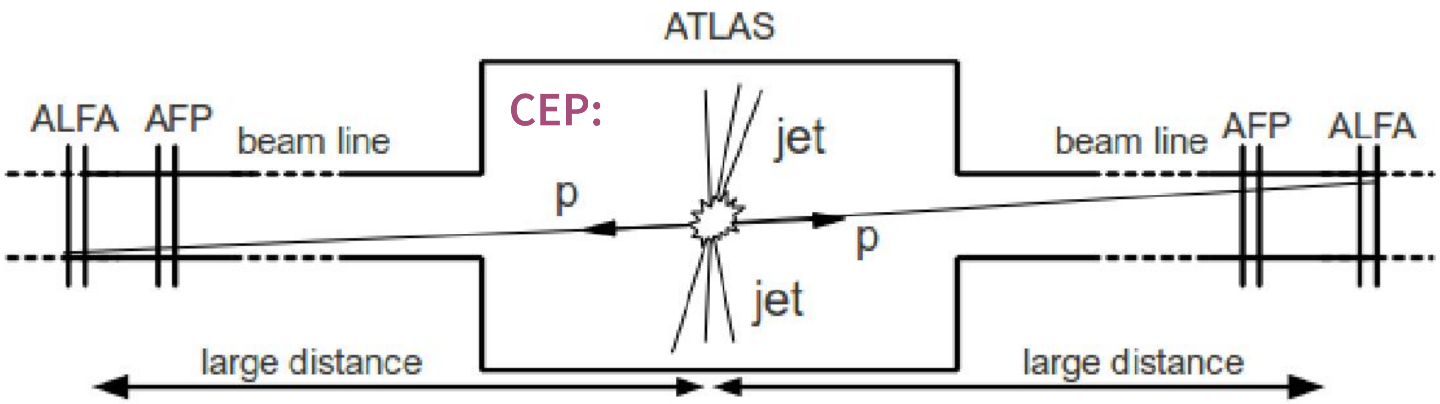

Figure from M. Trzebiński, CERN Detector Seminar (2017)

- ALFA: Absolute Luminosity For Atlas [JINST **11** P11013]
- AFP: Atlas Forward Proton [ATLAS-TDR-024]
    - Study performed by Marek Tasevsky [EPJC 83, 35 (2023)]

QCD Instanton Searches With Forward Proton Tags

Tasevsky *et al.* looked at ATLAS sensitivity to M > 60 GeV instantons in AFP-tagged events

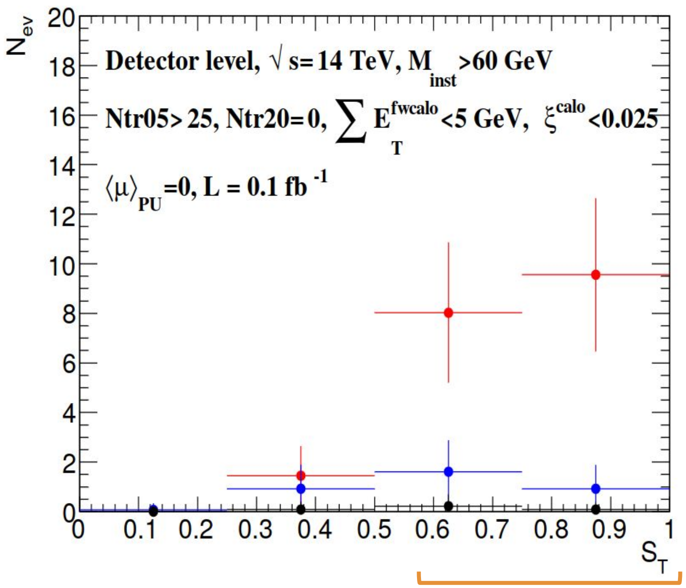

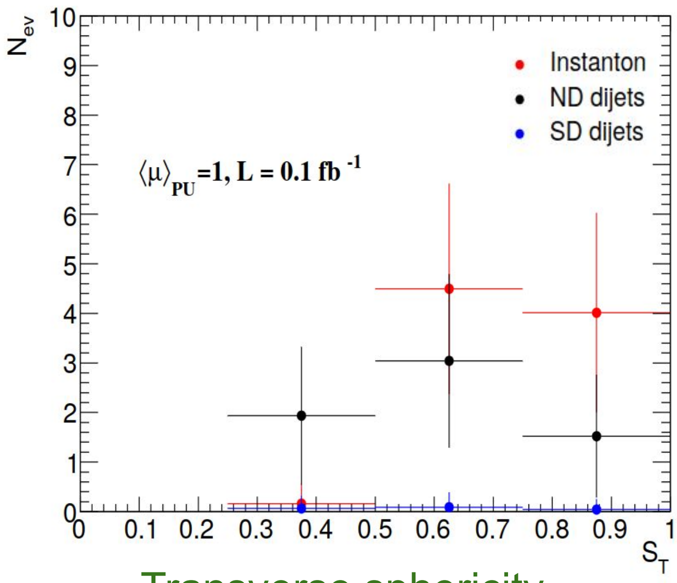

S / B > 1!

A very comprehensive study, considering single and double-AFP tags • four luminosity scenarios • multi-parton interactions • pile-up and combinatorial background protons • plus efficiency reductions from detector effects.

A Note on Theory Systematics

- Factorisation scale uncertainty
  - Factor of $2^{\pm 1}$ variations
  - Comparison with alternative choice, $\sqrt{\hat{s}}$ / N_{gluons}
- Renormalisation scale uncertainty
  - Implement custom μ_R reweighting in MC

$$\frac{(\mu_{\rm r}^{v})^{2b_0}}{(\mu_{\rm r}^{0})^{2b_0}}\,\frac{\exp\left[-4\pi/\alpha_S(\mu_{\rm r}^{v})\right]}{\exp\left[-4\pi/\alpha_S(\mu_{\rm r}^{0})\right]}$$

- Uncertainty on order of α_S
  - Somewhat captured by α_S variations and different PDF sets

In principle, there is an *O*(100) uncertainty on the instanton cross-section [2101.02719]

(but this is why we should measure it!)

Conclusion

- ATLAS search for QCD instantons is underway
  - But struggles with background modelling and rejection
- Can we improve our strategy?
  - Use forward proton tags
  - Use flavour tagging?
  - Target the chirality violation?

▶ Are there QCD instantons…?

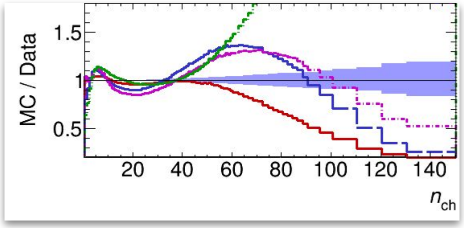

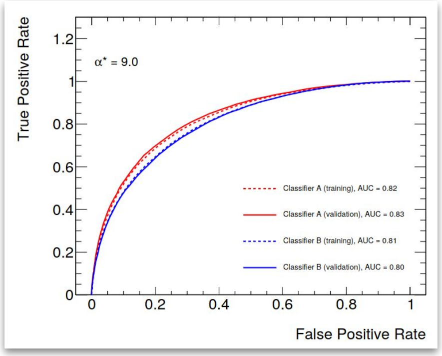

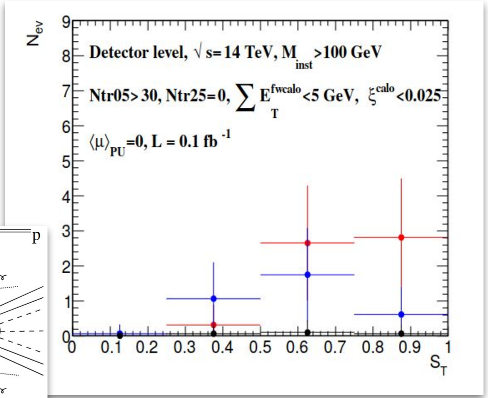

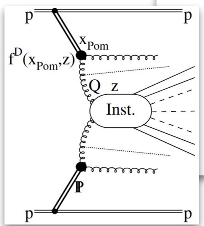

BACKUP

Much of My PhD Experience

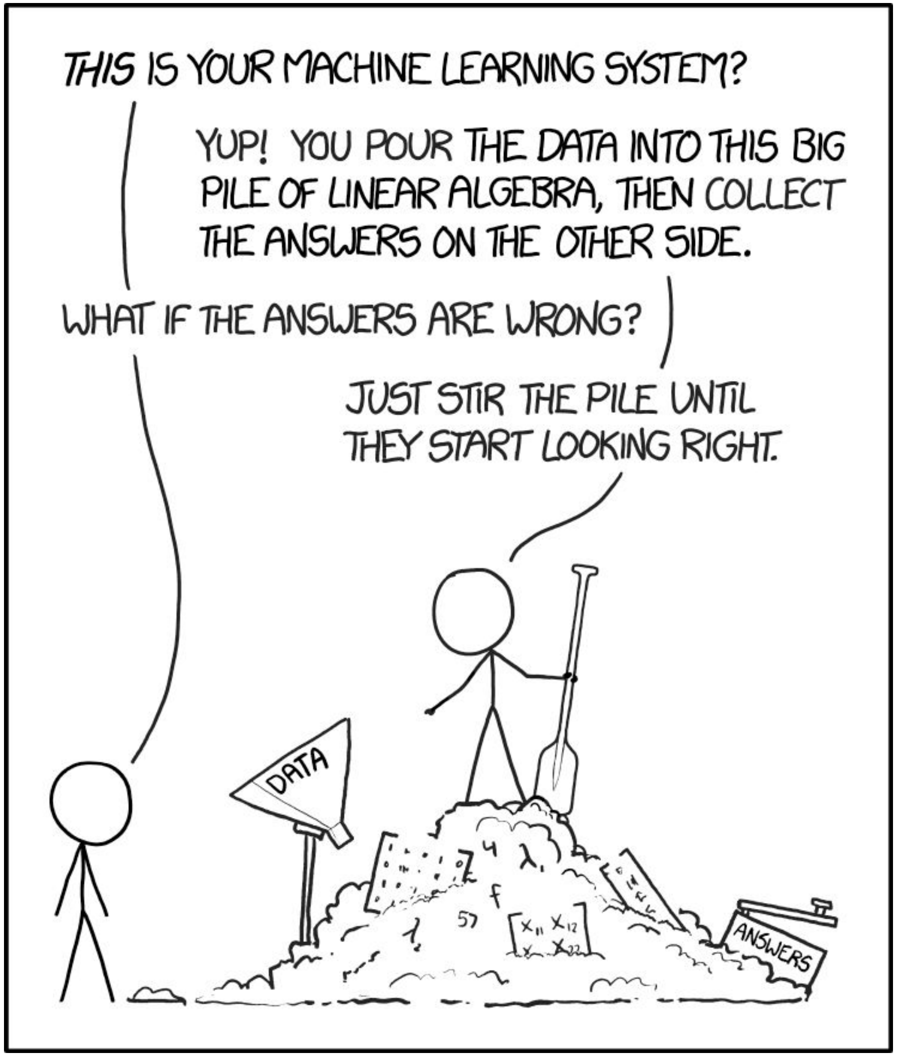

The ATLAS Experiment (A Toroidal LHC Apparatus)

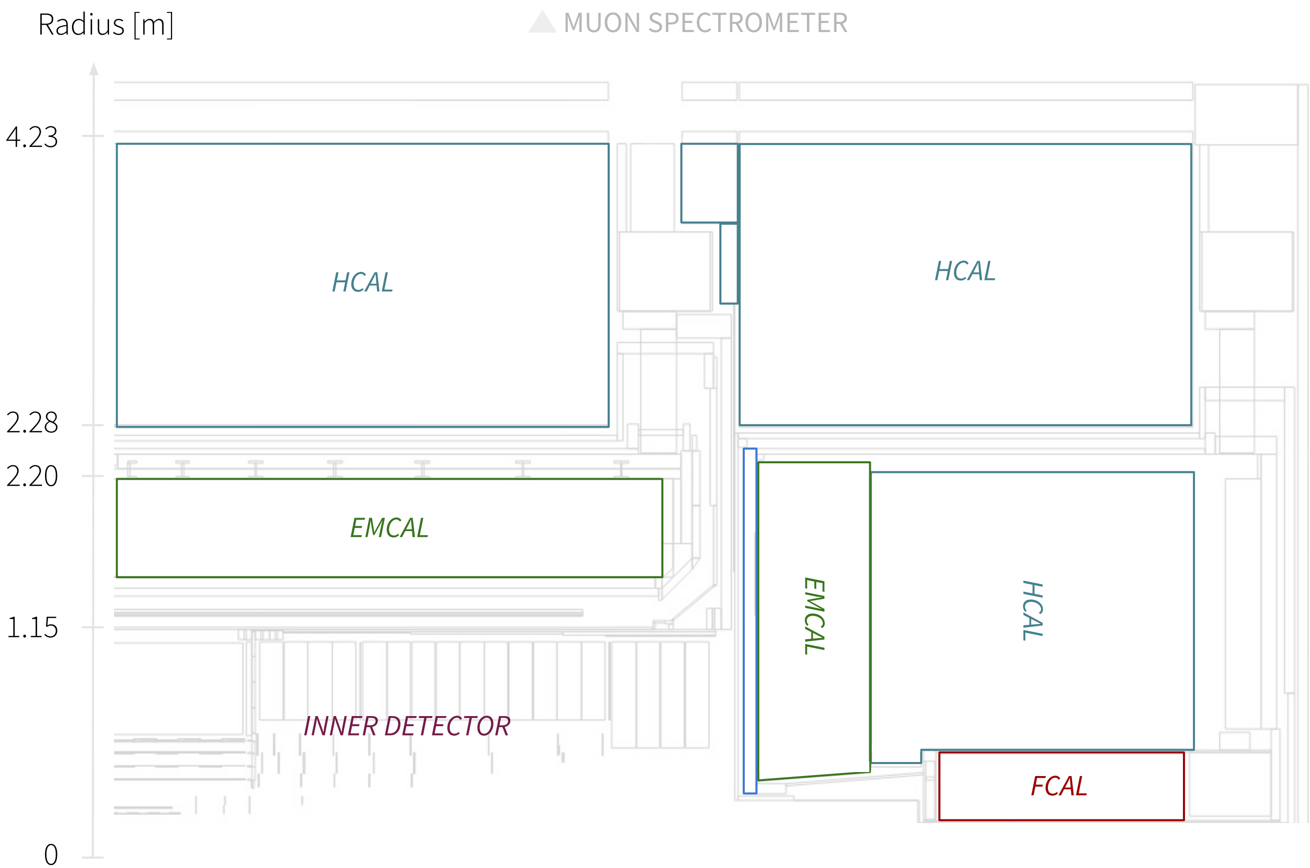

Muon Spectrometer

Precision trackers (MDTs, CSCs)

Fast trackers (RPCs, TGCs)

Barrel Hadronic Calorimeter (HCal)

Steel and scintillator tiles

Electromagnetic Calorimeter (EMCal)

Lead–LAr, accordion geometry

End-Cap Hadronic Calorimeter

Copper–LAr

Forward Calorimeter (FCal)

Copper/Tungsten–LAr

Inner Detector

Silicon pixels (Pixel detector)

Silicon microstrips (SCT)

Straws (TRT)

Minimum Bias Trigger Scintillators (MBTS)

Hodoscopes at $z = \pm 3.6$ m for triggering

[Detector paper (2008), Higgs boson discovery (2012), 1000 publications (2021)]

Previous ATLAS Soft QCD Measurements

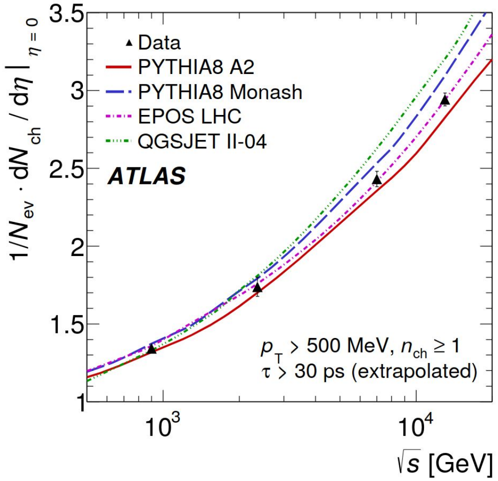

Minimum Bias (MB)

13 TeV, tracks-based: 1602.01633

13 TeV, 100 MeV tracks-based: 1606.01133

≤ 7 TeV, tracks-based: 1012.5104, etc.

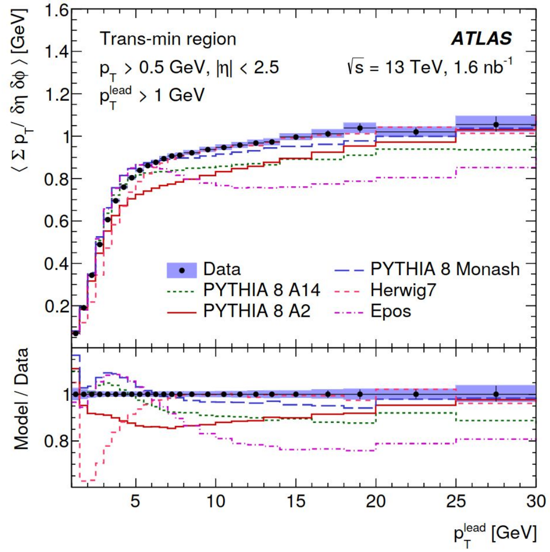

Underlying Event (UE)

13 TeV, tracks-based: 1701.05390

13 TeV in Z-events: 1905.09752

7 TeV with jets: 1406.0392, etc.

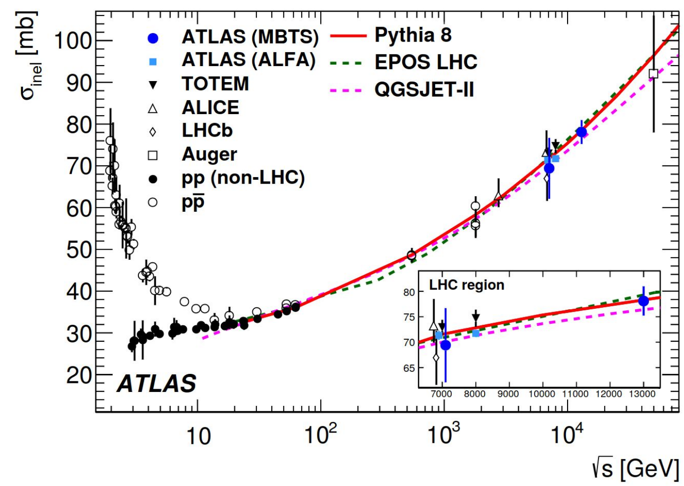

Total Inelastic *pp* Cross-Section

@ 13 TeV: 1606.02625

@ 7 TeV: 1104.0326, etc.

Performed for insights into low energy strong interactions

(Inputs to MC event generator tuning, understanding for pileup modelling, *etc.*)

Tracking Systematics

Impact parameter resolution

- Smear d0 and z0 within resolution
- \+ TRK_RES_D0_MEAS
- \+ TRK_RES_Z0_MEAS

Residual alignment uncertainties

- Use central η–ϕ maps of the residual biases
- \+ TRK_BIAS_D0_WM
- \+ TRK_BIAS_Z0_WM
- \+ TRK_BIAS_QOVERP_SAGITTA_WM

Efficiency uncertainties

- Account for difference of efficiency in data/MC from material uncertainty, based on truth-matching
- \+ TRK_EFF_<WP>_OVERALL
- \+ TRK_EFF_<WP>_IBL
- \+ TRK_EFF_<WP>_pp0
- \+ TRK_EFF_<WP>_PHYSMODEL

$$\epsilon_{\mathrm{trk}} = \frac{N_{\mathrm{rec}}^{\mathrm{matched}}(p_T, \eta)}{N_{\mathrm{gen}}(p_T, \eta)}$$

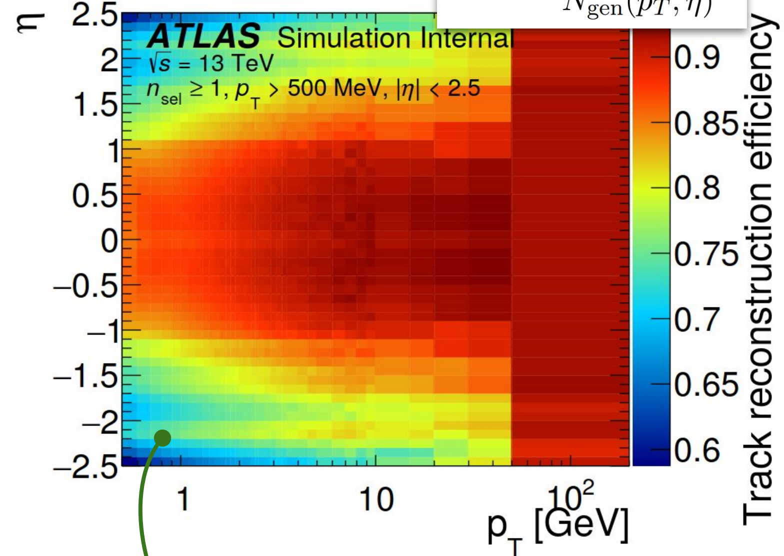

Make map like this for each material variation, then calculate

$$\sigma_{\mathrm{sys}} = \frac{\epsilon_{\mathrm{trk}}^{\mathrm{default}}(p_T, \eta)}{\epsilon_{\mathrm{trk}}^{\mathrm{varied}}(p_T, \eta)} - 1$$

Efficiency of the Single-Arm Minimum Bias Trigger

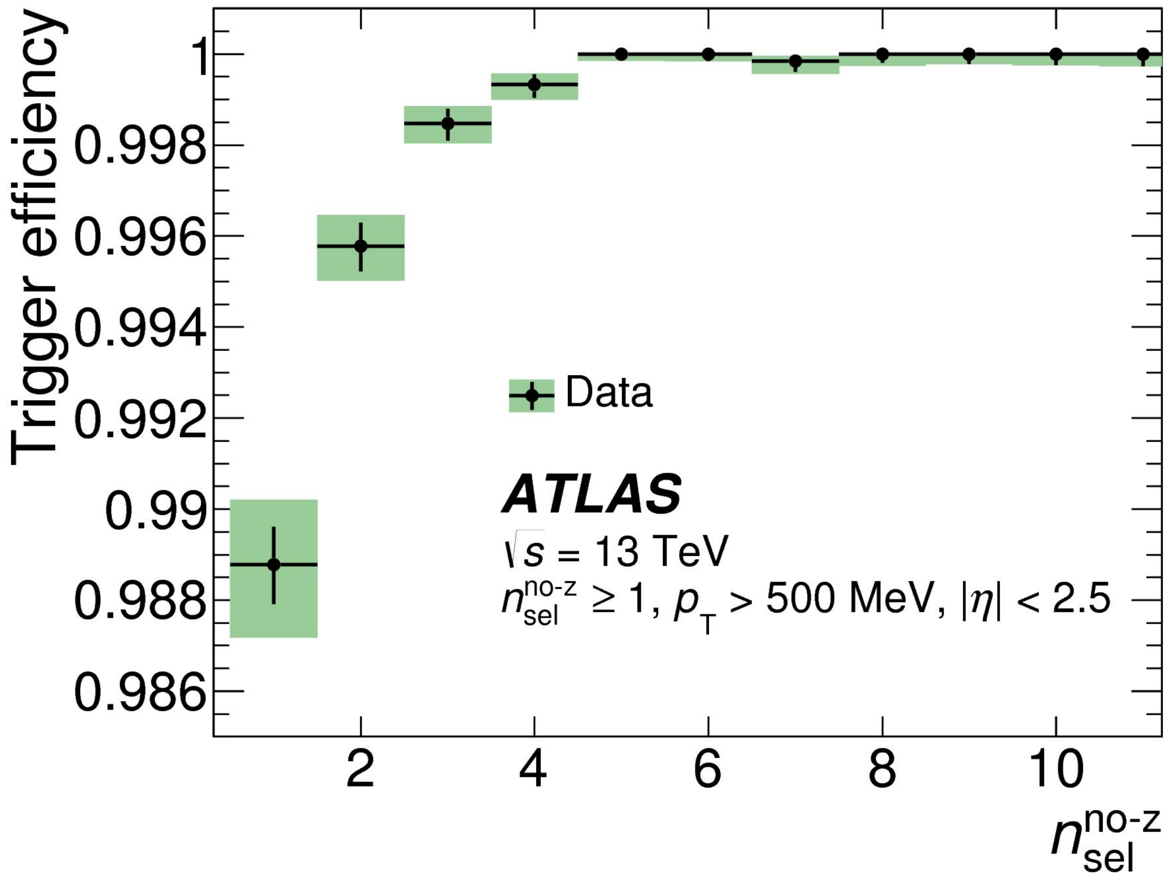

1602.01633

Signal-Modelling Systematics

Assess by performing reasonable variations of the event generation, e.g.

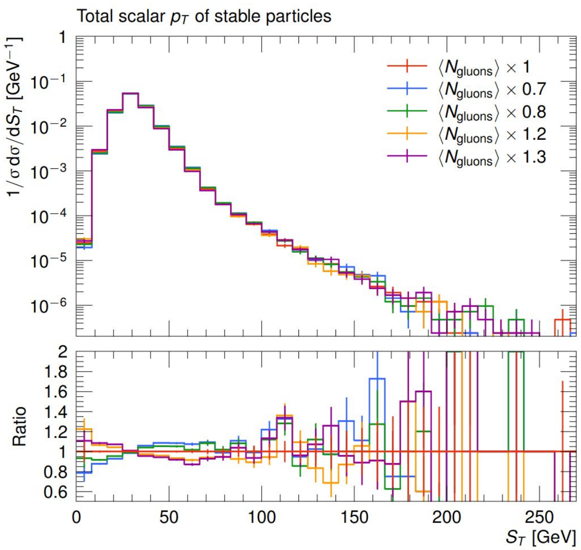

INSTANTON_NGLUONS_MODIFIER

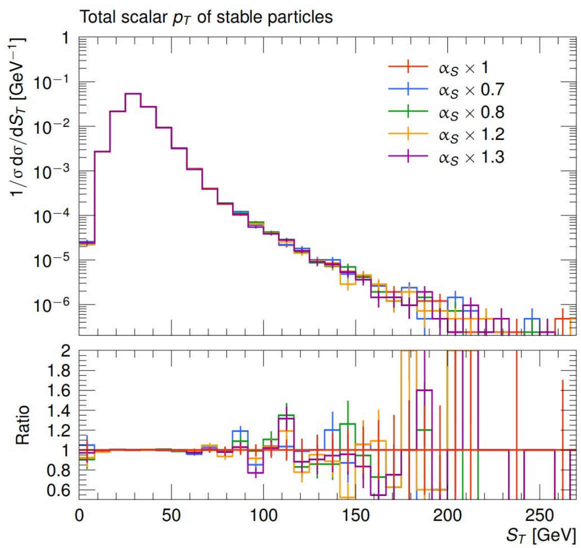

INSTANTON_ALPHAS_FACTOR

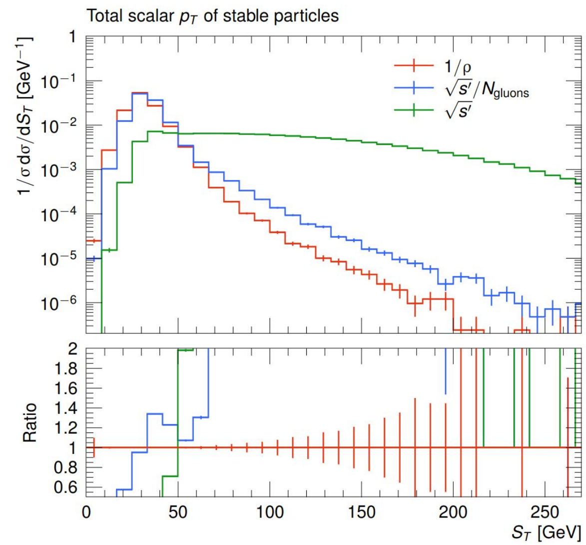

INSTANTON_SCALE_CHOICE

Small **Big**

- Not sure how to treat the scale choice variation ($1 / \rho \rightarrow \sqrt{s'} / N_{gluons}$), which is large
  - In principle the signal cross-section and its shape have to be recalculated

Flatenicity Calculated on a 10 x 10 Grid in η x ϕ

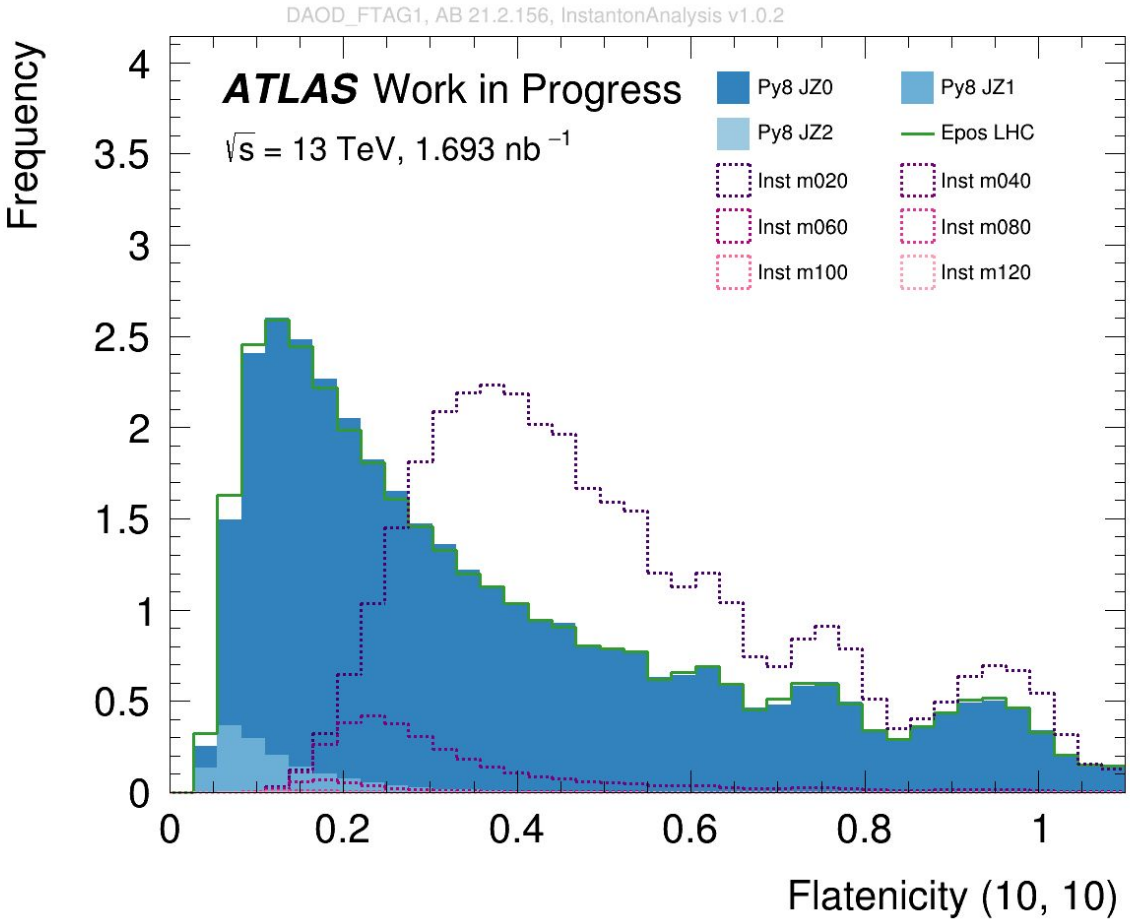

What Does a DNN Learn?

Look at 2d classifier output vs input histograms, e.g.

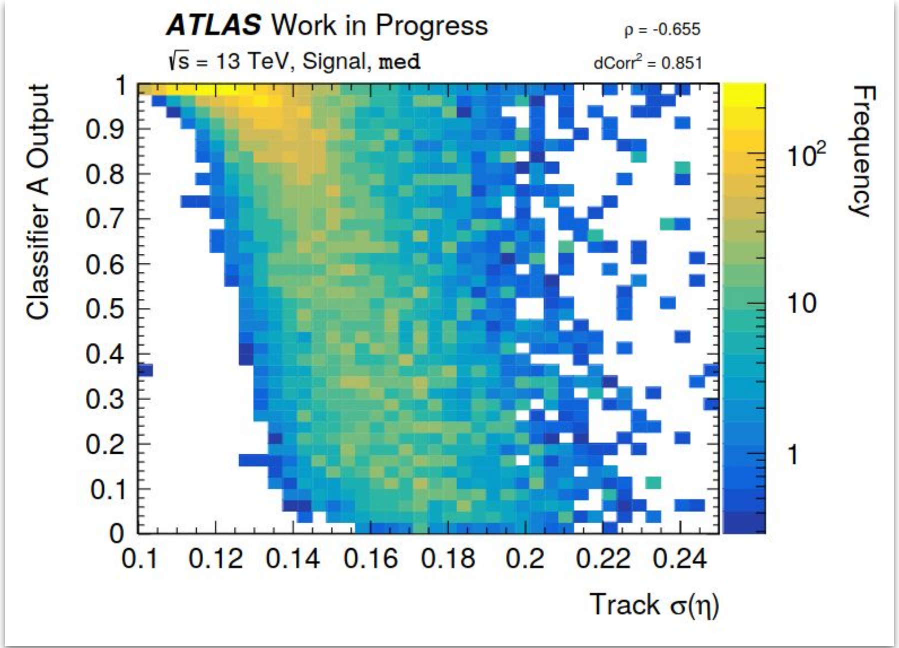

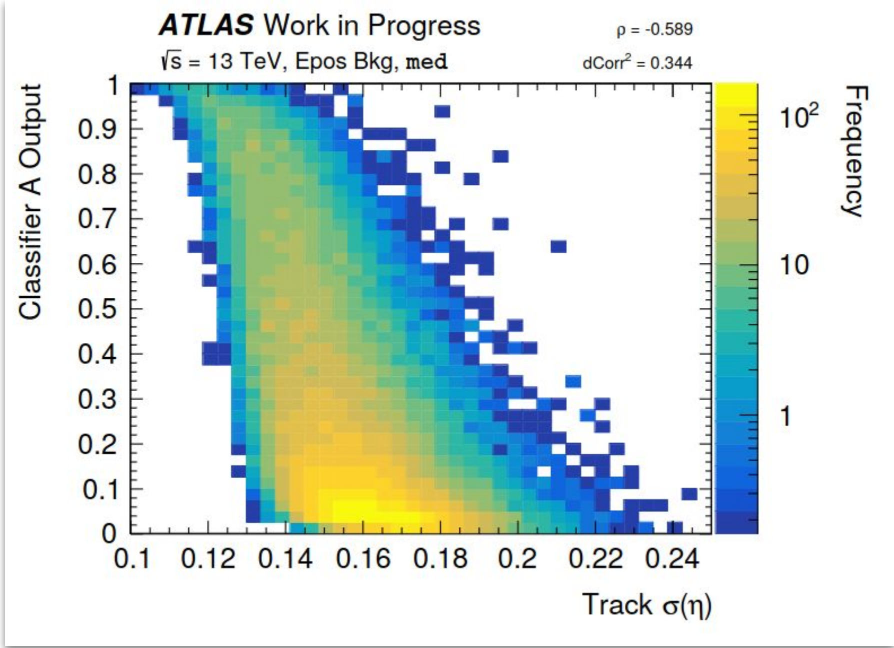

What Does a DNN Learn?

Even better: look at the profiles of the classifier outputs in classifier inputs, e.g.

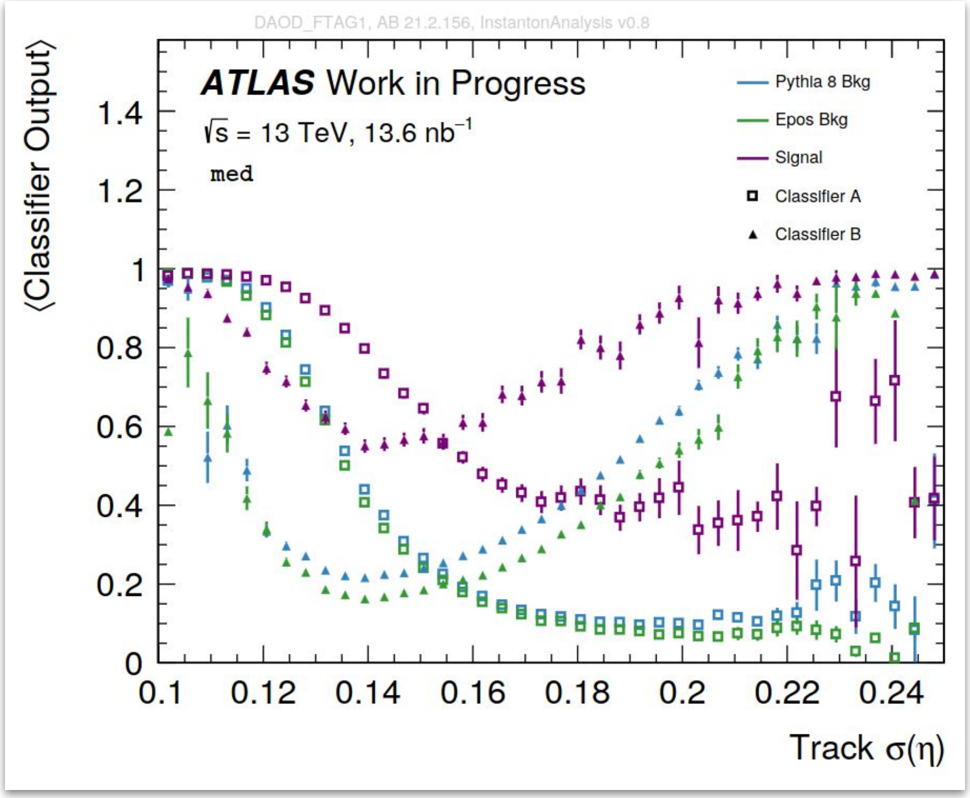

- Show that classifiers A and B make different use of the input variables
- Show where discrimination power comes from, e.g. here — edges vs center of track σ(η)

SHERPA UE Tuning: Models

Module	Model parameter
`AMISIC`	$p_{T,\mathrm{min}}$ $p_{T,\,0}$ ξ f_{mat} r_1 r_2
`Primordial_KPerp`	$\langle k_T \rangle$ σ k_T^{max} η α
`AHADIC`	

Sj\”ostrand–van Zijl model [Phys. Rev. **D** 36, 2019]

$$P_{\mathrm{no}}(p_{T,\mathrm{min}}) = \exp\left(-\frac{1}{\xi \sigma_{\mathrm{ND}}} \int_{p^2_{T,\mathrm{min}}} dp_T^2 \frac{d\hat{\sigma}}{dp_T^2} \right)$$

Transverse momentum regulator

$$p_T^2 \to p_T^2 + p_{T,0}^2$$

Double Gaussian matter density profile assumption

$$\rho(r) \propto (1 - f_{\mathrm{mat}}) \frac{1}{r_1^3} \exp\left(-\frac{r^2}{r_1^2} \right) + f_{\mathrm{mat}} \frac{1}{r_2^3} \exp\left(-\frac{r^2}{r_2^2} \right)$$

Intrinsic transverse momentum of partons in hadrons

$$\Pr(k_T) \propto \exp\left(-\frac{(k_T - \langle k_T \rangle)^2}{\sigma^2} \right) \times \left[1 - \left(\frac{k_T}{k_T^{\mathrm{max}}} \right)^{\eta} \right]$$

AHADIC model: *A modified cluster-hadronization model,* 0311085

Sherpa 2.2 manual, 1905.09127

SHERPA UE Tuning: 7 TeV Results in Pictures (1/3)

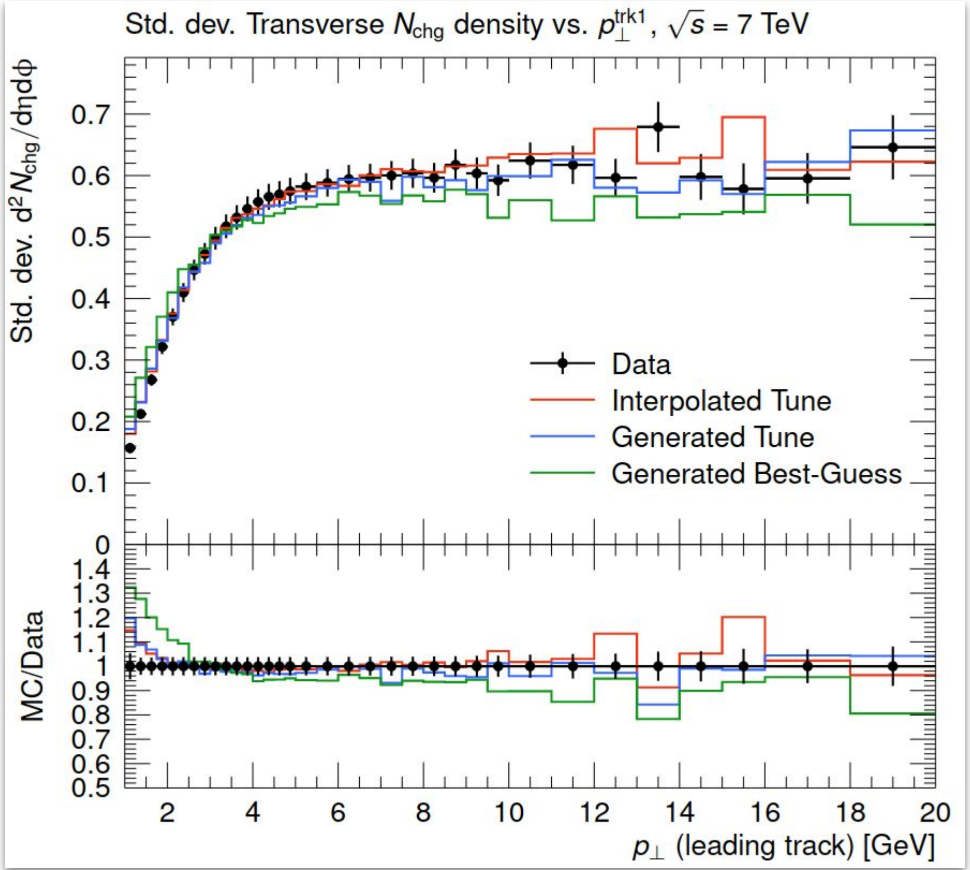

Tracks-based UE at 7 TeV ✔

[ATLAS_2010_S889472, 1012.0791]

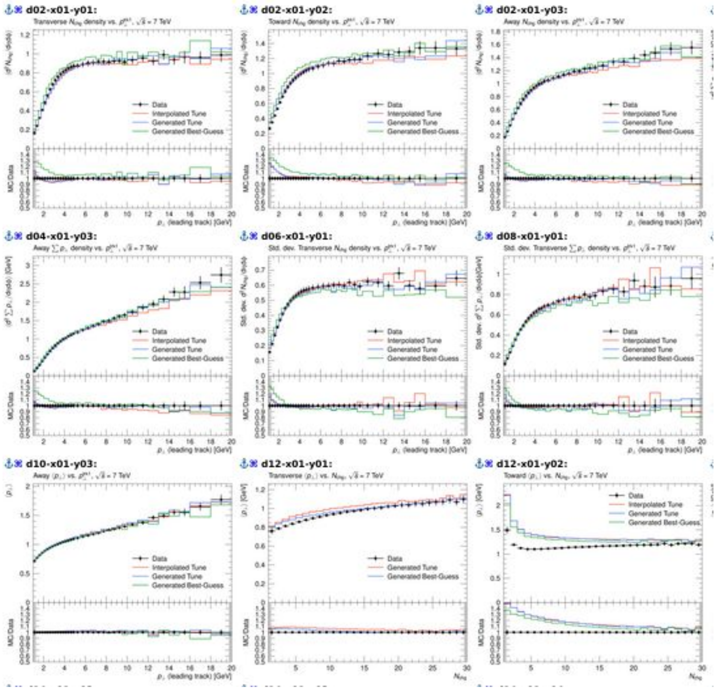

SHERPA UE Tuning: 7 TeV Results in Pictures (2/3)

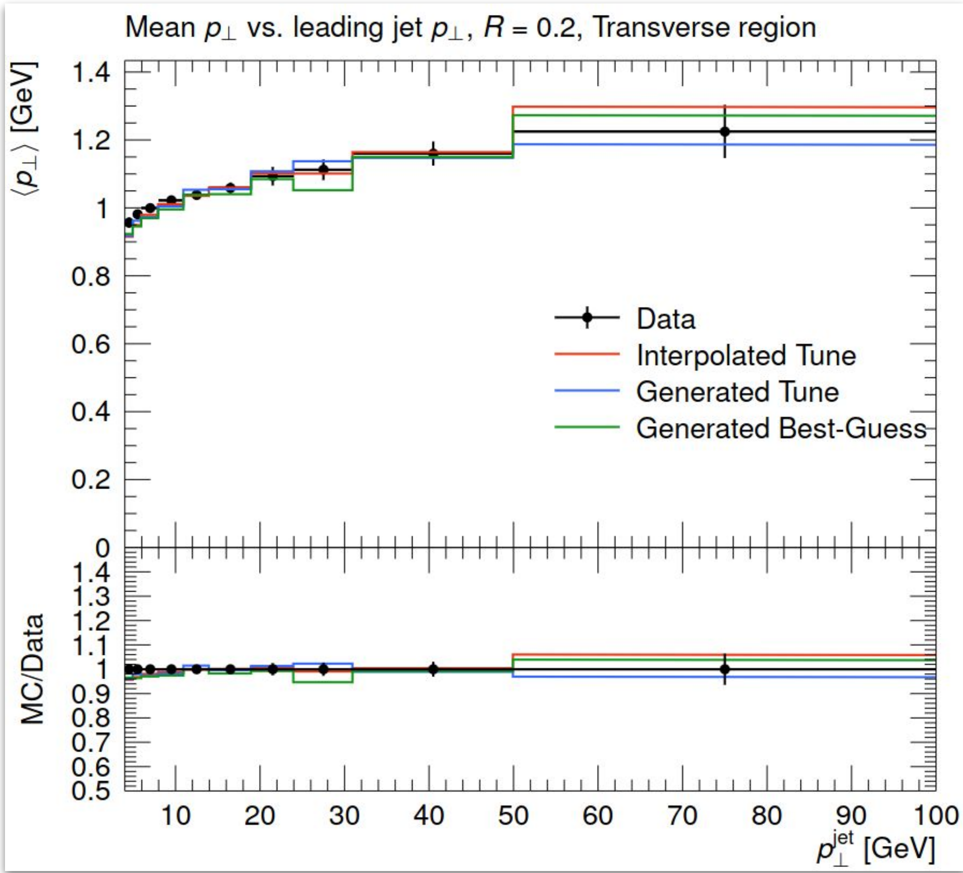

UE at 7 TeV with track-jets ✔

[ATLAS_2012_I1125575,1208.0563]

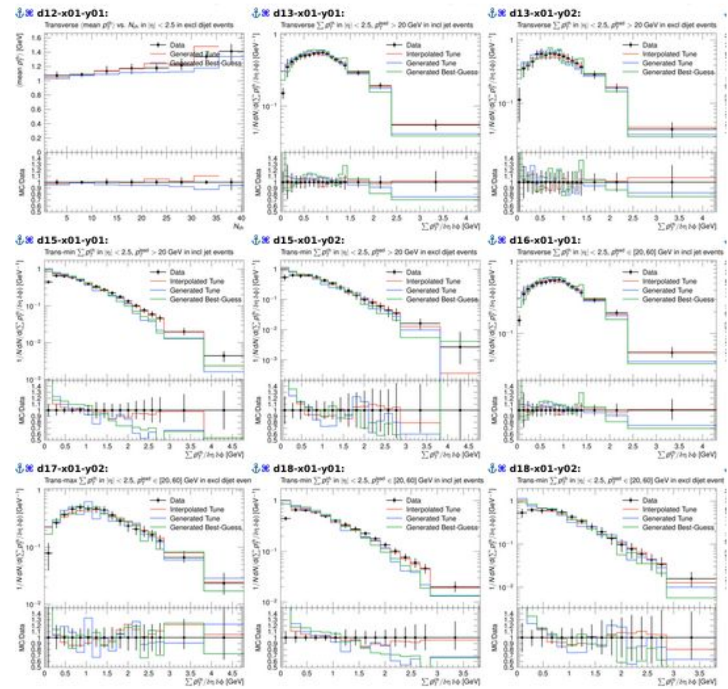

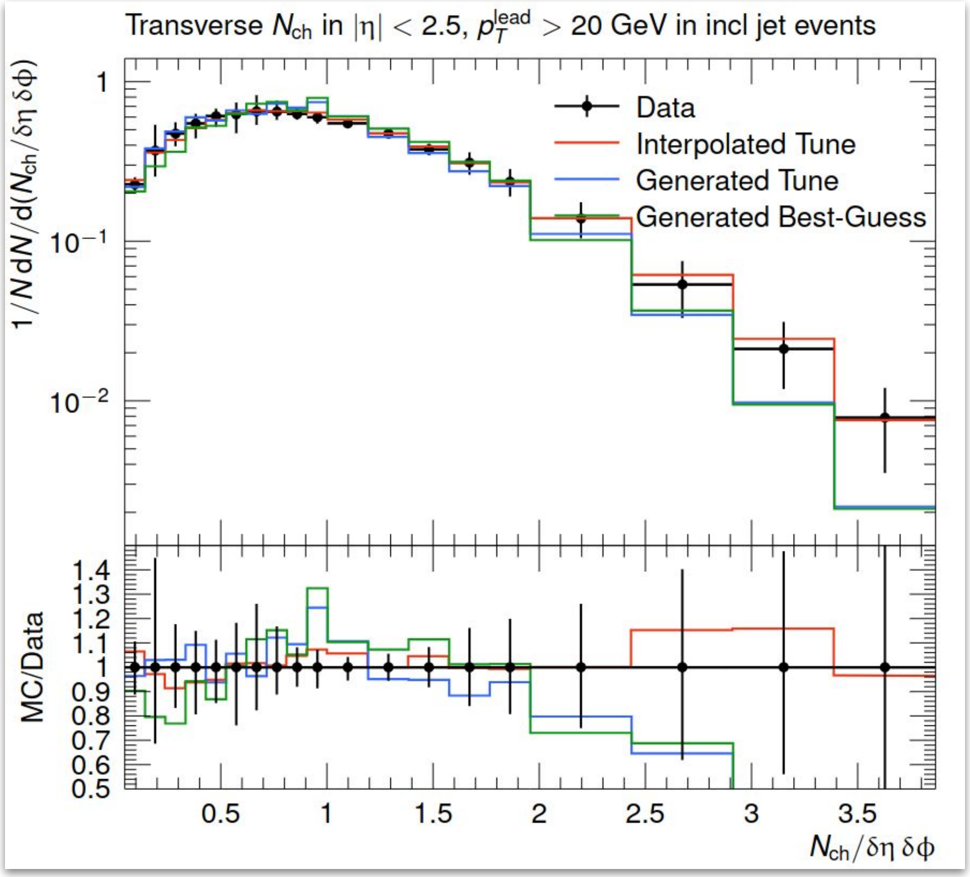

UE at 7 TeV with leading jet ✔

[ATLAS_2014_I1298811, 1406.0392]

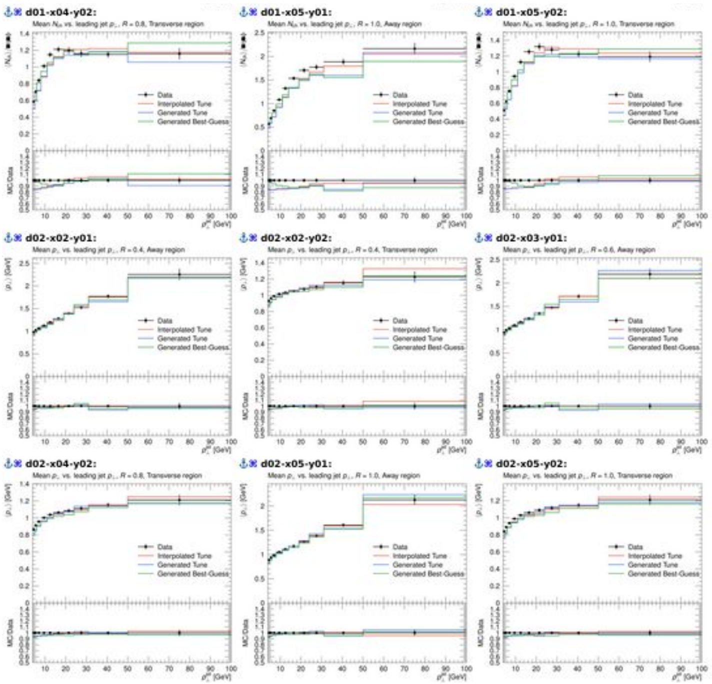

Fitted SHERPA UE Parameters

Parameter	Prior Value	Scan Range	Tuned Value	Relative Change
AMISIC::PT_0(ref)	2.5	0.1 – 1	0.716 ± 0.008	−71.4%
AMISIC::PT_Min(ref)	3	2.5 – 5	4.260 ± 0.009	+42.0%
AMISIC::SIGMA_ND_NORM	0.4	0.4 – 1	0.458 ± 0.003	+14.5%
AMISIC::MATTER_FRACTION1	0.5	0.1 – 0.4	0.187 ± 0.003	−62.6%
AMISIC::RADIUS1	0.4	0.0 – 0.5	0.157 ± 0.002	−60.8%
AMISIC::RADIUS2	1	0.8 – 1.5	0.890 ± 0.005	−11.0%
AMISIC::Eta	0.16	—	0.16	
INTRINSIC_KPERP::MEAN	0	0 – 1.2	1.004 ± 0.009	$+\infty$%
INTRINSIC_KPERP::SIGMA	1.5	0.5 – 3	1.10 ± 0.03	−27%
INTRINSIC_KPERP::MAX	3	2 – 5	2.69 ± 0.03	−10%
INTRINSIC_KPERP::CUT_EXPO	5	3 – 6	5.12 ± 0.04	+2%
AHADIC::ALPHA_B	2.5	—	15	
AHADIC::BETA_B	0.25	—	0.9	
AHADIC::GAMMA_B	0.5	—	15	

Phys. J. C 76 (2016) 7, 381

The background is modelled using the RAPGAP and DJANGOH Monte Carlo programs. The RAPGAP Monte Carlo program [32] incorporates the $\mathcal{O}(\alpha_s)$ QCD matrix elements and models higher order parton emissions to all orders in α_s using the concept of parton showers [33] based on the leading-logarithm DGLAP equations [34], where QCD radiation can occur before and after the hard subprocess. An alternative treatment of the perturbative phase is implemented in DJANGOH [35] which uses the Colour Dipole Model [36] with QCD matrix element corrections as implemented in ARIADNE [37]. In both MC generators hadronisation is modelled with the LUND string fragmentation [38, 39] using the ALEPH tune [40]. QED radiation and electroweak effects are simulated using the HERACLES [41] program, which is interfaced to the RAPGAP and DJANGOH event generators. The parton density functions of the proton are taken from the CTEQ6L set [42].

QCDINS [11, 43] is a Monte Carlo package to simulate QCD instanton-induced scattering processes in DIS. The hard process generator is embedded in the HERWIG [44] program and is implemented as explained in section 2. The number of flavours is set to $n_f = 3$. Outside the allowed region defined by $Q'^2_{\rm min}$ and $x'_{\rm min}$ the instanton cross section is set to zero. The CTEQ5L [45] parton density functions are employed[5]. Besides the hard instanton subprocess, subleading QCD emissions are simulated in the leading-logarithm approximation, using the coherent branching algorithm implemented in HERWIG. The hadronisation is performed according to the Lund string fragmentation.

Search at High-Q^2 by the H1 Collaboration

Phys. J. C 76 (2016) 7, 381

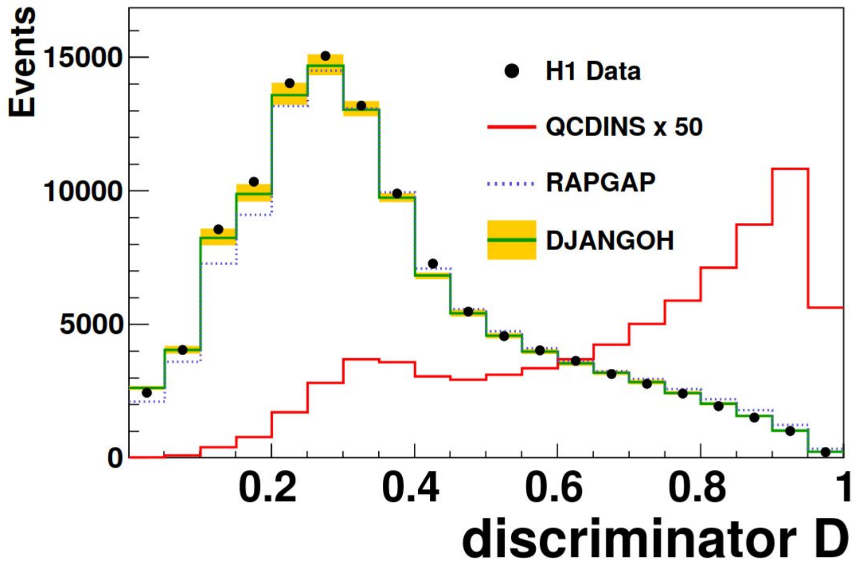

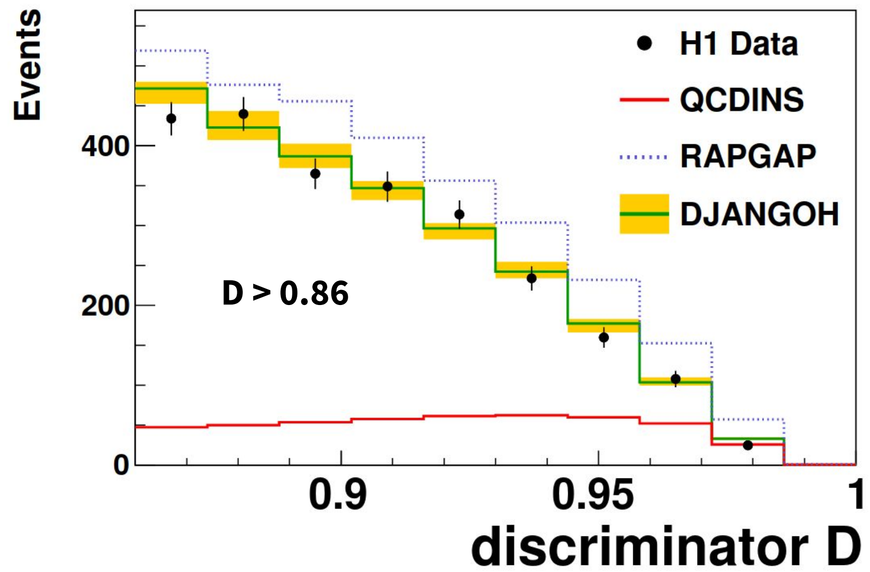

No evidence for QCD Instantons found, but predictions challenged for the first time.

Possibly not the final word from the HERA data...

Cross-sections of Central Instanton Production

V. V. Khoze *et al*, *Central Instanton Production*, 2111.02159

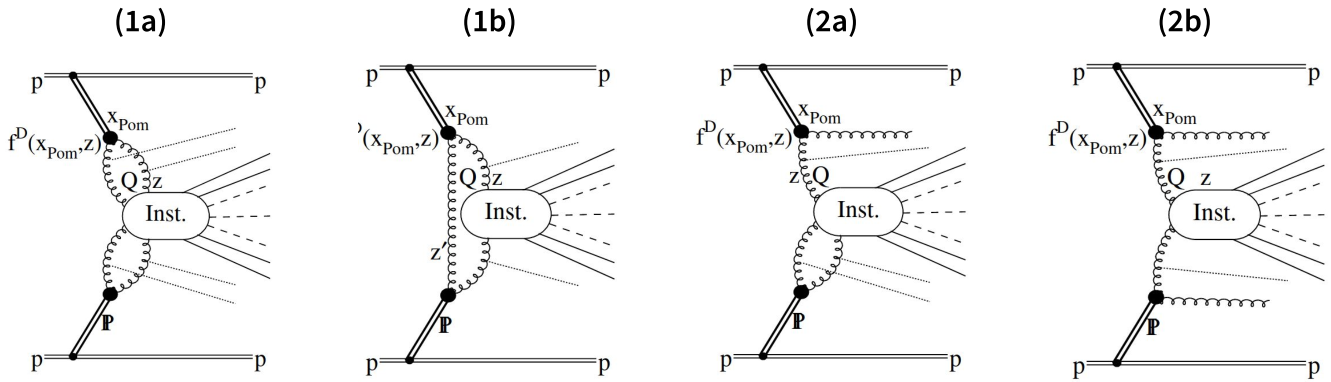

M_{inst} [GeV]	$d\sigma_{pp}^{(1a)}$[pb]	$d\sigma_{pp}^{(1b)}$[pb]	$d\sigma_{pp}^{(2a)}$[pb]	$d\sigma_{pp}^{(2b)}$[pb]	$d\sigma_{pp}^{(2b)}$, $Q_t > 20$GeV
15	13.3	$4.56{\cdot}10^{4}$	$3.72{\cdot}10^{3}$	$1.83{\cdot}10^{5}$	-
35	$6{\cdot}10^{-3}$	$1.69{\cdot}10^{2}$	8.10	$2.28{\cdot}10^{3}$	$1.99{\cdot}10^{-3}$
55	$3.82{\cdot}10^{-5}$	3.27	$1.19{\cdot}10^{-1}$	$8.96{\cdot}10^{1}$	$2.95{\cdot}10^{-3}$
75	$8.8{\cdot}10^{-7}$	$1.61{\cdot}10^{-1}$	$4.72{\cdot}10^{-3}$	7.06	$1.70{\cdot}10^{-3}$
95	$4.27{\cdot}10^{-8}$	$1.38{\cdot}10^{-2}$	$3.42{\cdot}10^{-4}$	$8.58{\cdot}10^{-1}$	$7.26{\cdot}10^{-4}$
115	$3.37{\cdot}10^{-9}$	$1.74{\cdot}10^{-3}$	$3.68{\cdot}10^{-5}$	$1.39{\cdot}10^{-1}$	$2.80{\cdot}10^{-4}$
135	$3.77{\cdot}10^{-10}$	$2.86{\cdot}10^{-4}$	$5.29{\cdot}10^{-6}$	$2.75{\cdot}10^{-2}$	$1.04{\cdot}10^{-4}$

Table 1: Instanton cross-sections at the 14 TeV LHC. The differential cross-sections for the process in Figs.1a, 1b and 2a, 2b, given by Eqs. (5.1) and (5.2), are computed for a range of instanton masses M_{inst}.

$(\langle\mu\rangle, \mathcal{L}[\text{fb}^{-1}])$	$M_{\text{inst}} > 60$ GeV	$M_{\text{inst}} > 100$ GeV
(0, 0.1)	19.0/(0.4+3.5)	5.8/(0.2+3.5)
(1.0, 0.1)	8.7/(6.5+0.2)	3.2/(4.7+0.2)
(2.0, 1.0)	52.2/(58.1+2.5)	15.4/(55.3+2.2)
(5.0, 10.0)	56.2/(205.6+13.3)	23.8/(137.1+7.6)

Table 1 Summary of event yields after applying cuts in Eq. (9) and Eq. (10) for the single-tag search approach for $M_{\text{inst}} > 60$ GeV and $M_{\text{inst}} > 100$ GeV, respectively, and for four luminosity scenarios $(\langle\mu\rangle, \mathcal{L})$. For each scenario, a ratio of number of signal to background events, $N_{\text{S}}/(N_{\text{ND}} + N_{\text{SD}})$, is shown.